

Blind Super-Resolution of Point Sources via Projected Gradient Descent

Sihan Mao and Jinchi Chen ^{*†}

June 7, 2022

Abstract

Blind super-resolution can be cast as a low rank matrix recovery problem by exploiting the inherent simplicity of the signal and the low dimensional structure of point spread functions. In this paper, we develop a simple yet efficient non-convex projected gradient descent method for this problem based on the low rank structure of the vectorized Hankel matrix associated with the target matrix. Theoretical analysis indicates that the proposed method exactly converges to the target matrix with a linear convergence rate under the similar conditions as convex approaches. Numerical results show that our approach is competitive with existing convex approaches in terms of recovery ability and efficiency.

1 Introduction

Blind super-resolution is the problem of estimating high-resolution information of a signal from its low-resolution measurements when the point spread functions (PSFs) are unknown. Such problem arises in a wide variety of applications, including seismic data analysis [25], nuclear magnetic resonance spectroscopy [27], multi-user communication system [23], and 3D single-molecule microscopy [28]. In particular, when the knowledge of PSFs is available, blind super-resolution reduces to the super-resolution problem [7, 8].

Without any additional assumptions, blind super-resolution of point sources is an ill-posed problem. To alleviate this issue, it is common to assume that the PSFs belong to a known low-dimensional subspace. Under this assumption and utilizing the lift technique, blind super-resolution of point sources can be formulated as a matrix recovery problem. By exploiting low dimensional structures of the target matrix, a series of works [15, 37, 21, 12, 31] theoretically studied under which conditions the target matrix can be recovered. The author in [15] considered the setting where the PSF is shared among all point sources, and established the recovery guarantees for the atomic norm minimization (ANM) method. Yang et al. [37] further studied the same method, but with multiple unknown PSFs. Li et al. [21] provided robust analysis of blind 1D super-resolution and later the work in [31] generalized [21] to 2D case. Recently, Chen et al. [12] proposed a nuclear norm minimization method based on the vectorized Hankel lift framework, which also appears in [38, 40] but for matrix completion. Moreover, [12] established the corresponding exact recovery guarantees. While strong theoretical guarantees have been built for blind super-resolution based on convex methods, these approaches are computational inefficient for the high dimensional setting. Therefore it is necessary to design efficient and provable algorithms to deal with the large-scale regime.

In the past few years, substantial progress has been made on designing and analyzing provable fast algorithms for applications from science and engineering via non-convex optimization [20, 13, 16], including

^{*}This work was supported by National Science Foundation of China under Grant No. 12001108. Parts of the results in this paper will be presented at the 2022 IEEE International Symposium on Information Theory [24].

[†]The authors are with School of Data Science, Fudan University, Shanghai, China (email: 18110980008@fudan.edu.cn; jcchen.phys@gmail.com)

matrix completion [14, 42], phase retrieval [29], blind deconvolution [22], spectrally sparse signal recovery [5, 6], to name just a few. The goal of this work is to develop an efficient non-convex algorithm for blind super-resolution problem.

1.1 Comparisons with Related Work and Main Contributions

Our work is closely related to [12, 5, 43]. As already mentioned, [12] proposed a convex approach called Vectorized Hankel Lift (VHL) for blind super-resolution. Based on this framework, we develop an efficient and provable non-convex algorithm for blind super-resolution of point sources. More precisely, we parameter the vectorized Hankel matrix corresponding to a candidate solution in terms of the Burer–Monteiro factorization and develop a projected gradient descent method to directly recover the low-rank factors.

Our algorithm is inspired by the method in [5], where the projected gradient descent was developed for spectrally sparse signal recovery problem based on the low rank structure of the Hankel matrix corresponding to the target signal. Despite this, both the structures of sensing operator and target matrix in this paper are substantially different from that in [5]. Therefore, the convergence analysis in [5] can not be easily extended to our model.

Recently, [43] follows our work and develops an iterative hard thresholding method based on the framework of vectorized Hankel lift to solve blind super-resolution problem. It is worth pointing out that they directly apply our result to bound the initialization error of their method. Furthermore, their proof idea is inspired by the guarantee analysis of low rank matrix recovery over Riemannian manifold [6, 36]. Therefore the proof techniques are totally different with ours.

The main contributions of this work are summarized as follows. Firstly, we present a new non-convex algorithm called projected gradient descent via vectorized Hankel lift (PGD–VHL) for blind super-resolution. Numerical experiments show that PGD–VHL is competitive with convex recovery methods such as ANM and VHL in terms of recovery ability, but is much more efficient. Secondly, we establish the recovery performance of PGD–VHL. Our results show that PGD–VHL started from a spectral initialization converges linearly to the target matrix under the similar sample complexity as convex approaches. Lastly, it is worth mentioning that the theoretical guarantee of PGD–VHL requires a slightly milder assumption on the low-dimensional subspace than that for VHL in [12].

1.2 Organization and Notation

The rest of this paper is organized as follows. Section 2 gives the problem setup of blind super-resolution of point sources. Section 3 presents the PGD–VHL algorithm whose the exact recovery guarantee is provided in Section 4. Numerical evaluations are presented to illustrate the performance of PGD–VHL in Section 5. All proofs are deferred to Section 6. Finally, we conclude this paper and propose some future work in Section 7.

Some notations used throughout this paper are presented as follows. Symbols for vectors, matrices and operators are in bold lowercase letters, bold uppercase letters and calligraphic letters, respectively. In this paper, vectors and matrices are indexed starting with zero. For a complex number x , its real part is denoted by $\Re(x)$. The transpose, complex conjugate, complex transpose, spectral norm and Frobenius norm of matrix \mathbf{X} are denoted as \mathbf{X}^\top , $\overline{\mathbf{X}}$, $\mathbf{X}^\mathbf{H}$, $\|\mathbf{X}\|$ and $\|\mathbf{X}\|_F$, respectively. The inner product of two matrices \mathbf{X}_1 and \mathbf{X}_2 is defined as $\langle \mathbf{X}_1, \mathbf{X}_2 \rangle = \text{trace}(\mathbf{X}_1^\mathbf{H} \mathbf{X}_2)$. Moreover, we will refer to $\mathbf{A} \odot \mathbf{B}$ and $\mathbf{A} \otimes \mathbf{B}$ as the Hadamard product and Kroncker product, respectively. We use $\mathbf{x}[\ell]$ to denote the ℓ -th entry of \mathbf{x} and $\mathbf{X}(j, :)$ to denote the j th row of \mathbf{X} . Moreover, we use the MATLAB notation $\mathbf{X}(i : j, k)$ to denote a vector of length $j - i + 1$, with entries $\mathbf{X}_{i,k}, \dots, \mathbf{X}_{j,k}$. The identity operator are denoted as \mathcal{I} . Let \mathcal{H} be the vectorized Hankel lift operator which maps a matrix $\mathbf{X} \in \mathbb{C}^{s \times n}$ into an $sn_1 \times n_2$ matrix,

$$\mathcal{H}(\mathbf{X}) = \begin{bmatrix} \mathbf{x}_0 & \mathbf{x}_1 & \cdots & \mathbf{x}_{n_2-1} \\ \mathbf{x}_1 & \mathbf{x}_2 & \cdots & \mathbf{x}_{n_2} \\ \vdots & \vdots & \ddots & \vdots \\ \mathbf{x}_{n_1-1} & \mathbf{x}_{n_1} & \cdots & \mathbf{x}_{n_1+n_2-1} \end{bmatrix} \in \mathbb{C}^{sn_1 \times n_2}, \quad (1.1)$$

where $\mathbf{x}_i \in \mathbb{C}^s$ is the i -th column of \mathbf{X} and $n_1 + n_2 = n + 1$. We denote the adjoint of \mathcal{H} by \mathcal{H}^* , which is a linear mapping from $\mathbb{C}^{s \times n_1 \times n_2}$ to $\mathbb{C}^{s \times n}$. In particular, for any matrix $\mathbf{Z} \in \mathbb{C}^{s \times n_1 \times n_2}$, the i -th column of $\mathcal{H}^*(\mathbf{Z})$ is given by

$$\mathcal{H}^*(\mathbf{Z})\mathbf{e}_i = \sum_{\substack{j+k=i \\ 0 \leq j \leq n_1-1, 0 \leq k \leq n_2-1}} \mathbf{z}_{j,k},$$

where $\mathbf{z}_{j,k}$ is the (j, k) -th block of \mathbf{Z} such that $\mathbf{z}_{j,k} = \mathbf{Z}(js : (j+1)s - 1, k)$. Letting $\mathcal{D}^2 = \mathcal{H}^*\mathcal{H}$, we have

$$\mathcal{D}^2(\mathbf{X}) = [w_0\mathbf{x}_0 \quad \cdots \quad w_{n-1}\mathbf{x}_{n-1}],$$

where the scale w_i is defined as

$$w_i = \#\{(j, k) | j+k = i, 0 \leq j \leq n_1 - 1, 0 \leq k \leq n_2 - 1\}.$$

Moreover, we define $\mathcal{G} = \mathcal{H}\mathcal{D}^{-1}$. The adjoint of \mathcal{G} denoted \mathcal{G}^* is given by $\mathcal{G}^* = \mathcal{D}^{-1}\mathcal{H}^*$. Additionally, \mathcal{G} and \mathcal{G}^* satisfy

$$\mathcal{G}^*\mathcal{G} = \mathcal{I}, \quad \|\mathcal{G}\| = 1, \quad \text{and} \quad \|\mathcal{G}^*\| \leq 1. \quad (1.2)$$

We use \mathbf{G}_i to denote the matrix defined by

$$\mathbf{G}_i = \frac{1}{\sqrt{w_i}} \sum_{\substack{j+k=i \\ 0 \leq j \leq n_1-1, 0 \leq k \leq n_2-1}} \mathbf{e}_j \mathbf{e}_k^\top. \quad (1.3)$$

Then one has

$$\mathcal{G}(\mathbf{X}) = \sum_{i=0}^{n-1} \mathcal{G}(\mathbf{x}_i \mathbf{e}_i^\top) = \sum_{i=0}^{n-1} \mathbf{G}_i \otimes \mathbf{x}_i, \quad (1.4)$$

where $\mathbf{G}_i \otimes \mathbf{x}_i$ denotes the Kronecker product between \mathbf{G}_i and \mathbf{x}_i .

Throughout this paper, c, c_0, c_1, \dots denote absolute positive numerical constants whose values may vary from line to line. The notation $n = \mathcal{O}(m)$ means that there exists an absolute constant $c > 0$ such that $n \leq cm$.

2 Problem formulation

The point source signal model can be represented as a superposition of r spikes

$$x(t) = \sum_{k=1}^r d_k \delta(t - \tau_k), \quad (2.1)$$

where $\delta(\cdot)$ is the Dirac function, $d_k \in \mathbb{C}$ and $\tau_k \in [0, 1)$ are the amplitude and location of the k -th point source, respectively. Let $\{g_k(t)\}_{k=1}^r$ be the unknown point spread functions depending on the locations of point sources. The observation is a convolution between $x(t)$ and $\{g_k(t)\}_{k=1}^r$, that is,

$$y(t) = \sum_{k=1}^r d_k \delta(t - \tau_k) * g_k(t) = \sum_{k=1}^r d_k \cdot g_k(t - \tau_k). \quad (2.2)$$

After taking the Fourier transform and sampling, we obtain the measurements as

$$\mathbf{y}[j] = \sum_{k=1}^r d_k e^{-2\pi i \tau_k \cdot j} \hat{g}_k[j], \quad j = 0, \dots, n-1. \quad (2.3)$$

Let $\mathbf{g}_k = [\hat{g}_k[0] \ \cdots \ \hat{g}_k[n-1]]^\top$ be a vector corresponding to the k -th unknown point spread function. The goal is to estimate $\{d_k, \tau_k\}_{k=1}^r$ as well as $\{\mathbf{g}_k\}_{k=1}^r$ from (2.3).

Obviously, the problem of blind super-resolution is ill-posed without any additional assumptions, because the number of unknowns in (2.3) is $\mathcal{O}(nr)$, which is larger than the number of samples n . To tackle this issue, we follow the same route as that in [1, 15, 37, 12] and assume that all the Fourier samples of the unknown PSFs $\{\mathbf{g}_k\}_{k=1}^r$ belong to a known low-dimensional subspace spanned by the columns of $\mathbf{B} \in \mathbb{C}^{n \times s}$ with $s < n$, i.e.,

$$\mathbf{g}_k = \mathbf{B}\mathbf{h}_k, \quad (2.4)$$

where $\mathbf{h}_k \in \mathbb{C}^s$ denotes the unknown directional vector of \mathbf{g}_k in the subspace. According to the subspace assumption (2.4) and using the lift trick [1], we can easily rewrite (2.3) as a set of linear measurements with respect to the target matrix $\mathbf{X}^\natural = \sum_{k=1}^r d_k \mathbf{h}_k \mathbf{a}_{\tau_k}^\top$,

$$\mathbf{y}[j] = \langle \mathbf{b}_j \mathbf{e}_j^\top, \mathbf{X}^\natural \rangle, \quad j = 0, \dots, n-1, \quad (2.5)$$

where $\mathbf{a}_{\tau_k} = [1, e^{-2\pi i \tau_k}, \dots, e^{-2\pi i \tau_k \cdot (n-1)}]^\top$, $\mathbf{b}_j \in \mathbb{C}^s$ is the j th column vector of $\mathbf{B}^\mathbf{H}$, \mathbf{e}_j is the j -th standard basis of \mathbb{R}^n . The measurement model (2.5) can be rewritten succinctly as

$$\mathbf{y} = \mathcal{A}(\mathbf{X}^\natural), \quad (2.6)$$

where $\mathcal{A} : \mathbb{C}^{s \times n} \rightarrow \mathbb{C}^n$ is the linear operator. Let \mathcal{A}^* be the adjoint operator of \mathcal{A} which is given by $\mathcal{A}^*(\mathbf{y}) = \sum_{j=0}^{n-1} \mathbf{y}[j] \mathbf{b}_j \mathbf{e}_j^\top$. Furthermore, define $\mathbf{D} = \text{diag}(\sqrt{w_0}, \dots, \sqrt{w_{n-1}})$. We have $\mathbf{D}\mathcal{A}(\mathbf{X}) = \mathcal{A}\mathbf{D}(\mathbf{X})$ for any \mathbf{X} . The measurements can be reformulated as

$$\mathbf{D}\mathbf{y} = \mathcal{A}\mathbf{D}(\mathbf{X}^\natural). \quad (2.7)$$

Note that once the data matrix \mathbf{X}^\natural is reconstructed, the frequencies $\{\tau_k\}_{k=1}^r$ can be retrieved through spatial smoothing MUSIC [18, 17, 39, 12], and the amplitudes $\{d_k\}_{k=1}^r$ and coefficients $\{\mathbf{h}_k\}_{k=1}^r$ can be estimated by solving an over-determined linear system. Therefore in this work we focus on the problem of recovering \mathbf{X}^\natural from its linear measurements (2.6).

It has been shown that $\mathcal{H}(\mathbf{X}^\natural)$ is a rank- r matrix [12] and thus the matrix $\mathcal{H}(\mathbf{X}^\natural)$ admits low rank structure when $r \ll \min(sn_1, n_2)$. Equipped with the low rank structure of $\mathcal{H}(\mathbf{X}^\natural)$, it is natural to recover \mathbf{X}^\natural by solving the constrained least squares problem

$$\min_{\mathbf{X}} \frac{1}{2} \|\mathbf{D}\mathbf{y} - \mathcal{A}\mathbf{D}(\mathbf{X})\|_2^2 \quad \text{s.t.} \quad \text{rank}(\mathcal{H}(\mathbf{X})) = r. \quad (2.8)$$

Letting $\mathbf{Z} = \mathcal{H}(\mathbf{X}) = \mathcal{G}\mathbf{D}(\mathbf{X})$ for any \mathbf{X} , it can be verified that $(\mathcal{I} - \mathcal{G}\mathcal{G}^*)(\mathbf{Z}) = \mathbf{0}$. To eliminate the rank constrain in (2.8), we apply the Burer–Monteiro factorization [4] to parameterize \mathbf{Z} as $\mathbf{Z} = \mathbf{L}\mathbf{R}^\mathbf{H}$, where $\mathbf{L} \in \mathbb{C}^{sn_1 \times r}$ and $\mathbf{R} \in \mathbb{C}^{n_2 \times r}$ are two rank- r matrices. Therefore, the optimization problem (2.8) can be rewritten as

$$\min_{\mathbf{L}, \mathbf{R}} \frac{1}{2} \|\mathbf{D}\mathbf{y} - \mathcal{A}\mathcal{G}^*(\mathbf{L}\mathbf{R}^\mathbf{H})\|_2^2 \quad \text{s.t.} \quad (\mathcal{I} - \mathcal{G}\mathcal{G}^*)(\mathbf{L}\mathbf{R}^\mathbf{H}) = \mathbf{0}. \quad (2.9)$$

Before introducing our algorithm, we make an assumption that $\mathbf{Z}^\natural = \mathcal{H}(\mathbf{X}^\natural)$ is μ_1 -incoherent which is defined below.

Assumption 2.1. Let $\mathbf{Z}^\natural = \mathbf{U}\mathbf{\Sigma}\mathbf{V}^\mathbf{H}$ be the singular value decomposition of \mathbf{Z}^\natural , where $\mathbf{U} \in \mathbb{C}^{sn_1 \times r}$, $\mathbf{\Sigma} \in \mathbb{R}^{r \times r}$ and $\mathbf{V} \in \mathbb{C}^{n_2 \times r}$. Denote $\mathbf{U}^\mathbf{H} = [\mathbf{U}_0^\mathbf{H} \ \cdots \ \mathbf{U}_{n_1-1}^\mathbf{H}]^\mathbf{H}$, where $\mathbf{U}_j = \mathbf{U}[js : (j+1)s - 1, :]$ is the j -th block of \mathbf{U} for $j = 0, \dots, n_1 - 1$. The matrix \mathbf{Z}^\natural is μ_1 -incoherent if \mathbf{U} and \mathbf{V} obey that

$$\max_{0 \leq j \leq n_1 - 1} \|\mathbf{U}_j\|_F^2 \leq \frac{\mu_1 r}{n} \quad \text{and} \quad \max_{0 \leq k \leq n_2 - 1} \|\mathbf{e}_k^\top \mathbf{V}\|_2^2 \leq \frac{\mu_1 r}{n}$$

for some positive constant μ_1 .

Remark 2.1. Assumption 2.1 is the same as the one made in [11, 40] for low rank matrix recovery and is used in [12] for blind super-resolution. It has been established that Assumption 2.1 is obeyed when the minimum wrap-up distance between the locations of point sources is greater than about $2/n$.

Let μ and σ be two numerical constants such $\mu_1 \leq \mu$ and $\sigma_1 \leq \sigma$, and \mathcal{M} be a convex set defined as follows

$$\mathcal{M} = \left\{ \begin{bmatrix} \mathbf{L} \\ \mathbf{R} \end{bmatrix} : \max_{0 \leq j \leq n_1-1} \|\mathbf{L}_j\|_F \leq \sqrt{\frac{\mu r \sigma}{n}}, \|\mathbf{R}\|_{2,\infty} \leq \sqrt{\frac{\mu r \sigma}{n}} \right\}, \quad (2.10)$$

where \mathbf{L}_j is the j -th block of \mathbf{L} . Define

$$\mathbf{M}^\natural = \begin{bmatrix} \mathbf{L}^\natural \\ \mathbf{R}^\natural \end{bmatrix} = \begin{bmatrix} \mathbf{U}\Sigma^{1/2} \\ \mathbf{V}\Sigma^{1/2} \end{bmatrix}.$$

Since \mathbf{Z}^\natural is μ_1 -incoherent, we have $\mathbf{M}^\natural \in \mathcal{M}$. Therefore, we consider a penalized version of (2.9) for recovering the factorized matrices:

$$\min_{\mathbf{M} \in \mathcal{M}} \left\{ f(\mathbf{M}) := \frac{1}{2} \|\mathbf{D}\mathbf{y} - \mathcal{A}\mathcal{G}^*(\mathbf{L}\mathbf{R}^\mathbf{H})\|_2^2 + \frac{1}{2} \|(\mathcal{I} - \mathcal{G}\mathcal{G}^*)(\mathbf{L}\mathbf{R}^\mathbf{H})\|_F^2 + \frac{1}{16} \|\mathbf{L}^\mathbf{H}\mathbf{L} - \mathbf{R}^\mathbf{H}\mathbf{R}\|_F^2 \right\}, \quad (2.11)$$

where $\mathbf{M} = \begin{bmatrix} \mathbf{L}^\mathbf{H} & \mathbf{R}^\mathbf{H} \end{bmatrix}^\mathbf{H} \in \mathbb{C}^{(n_1+n_2) \times r}$, and the last term penalizes the mismatch between \mathbf{L} and \mathbf{R} , which is widely used in rectangular low rank matrix recovery [34, 42, 16].

3 Algorithm: projected gradient descent

Inspired by [5], we design a projected gradient descent method for the problem (2.11), which is summarized in Algorithm 1. The initialization involves two steps: (1) computes the best rank r approximation of $\mathcal{H}\mathcal{A}^*(\mathbf{y})$

Algorithm 1 PGD-VHL

Input: $\mathcal{A}, \mathbf{y}, n, s, r$

Initialization:

$$\widehat{\mathbf{Z}}_0 = \widehat{\mathbf{U}}_0 \widehat{\Sigma}_0 \widehat{\mathbf{V}}_0^\mathbf{H} = \mathcal{P}_r \mathcal{H}\mathcal{A}^*(\mathbf{y})$$

$$\widehat{\mathbf{L}}_0 = \widehat{\mathbf{U}}_0 \widehat{\Sigma}_0^{1/2}, \quad \widehat{\mathbf{R}}_0 = \widehat{\mathbf{V}}_0 \widehat{\Sigma}_0^{1/2}$$

$$\widehat{\mathbf{M}}_0 = \begin{bmatrix} \widehat{\mathbf{L}}_0^\mathbf{H} & \widehat{\mathbf{R}}_0^\mathbf{H} \end{bmatrix}^\mathbf{H}$$

$$(\mathbf{L}_0, \mathbf{R}_0) = \mathcal{P}_{\mathcal{M}}(\widehat{\mathbf{L}}_0, \widehat{\mathbf{R}}_0)$$

$$\mathbf{M}_0 = \begin{bmatrix} \mathbf{L}_0^\mathbf{H} & \mathbf{R}_0^\mathbf{H} \end{bmatrix}^\mathbf{H}$$

while not convergence **do**

$$\mathbf{M}_{t+1} = \mathcal{P}_{\mathcal{M}}(\mathbf{M}_t - \eta \nabla f(\mathbf{M}_t)).$$

end while

via one step hard thresholding $\mathcal{P}_r(\cdot)$, where \mathcal{A}^* is the adjoint of \mathcal{A} and $\mathcal{P}_r(\mathbf{Z})$ is the best rank r approximation of \mathbf{Z} ; (2) projects the low-rank factors of best rank- r approximated matrix onto the convex feasible set \mathcal{M} .

Given a matrix $\mathbf{M} = \begin{bmatrix} \mathbf{L}^\mathbf{H} & \mathbf{R}^\mathbf{H} \end{bmatrix}^\mathbf{H}$, the projection onto \mathcal{M} , denoted by $\begin{bmatrix} \widehat{\mathbf{L}}^\mathbf{H} & \widehat{\mathbf{R}}^\mathbf{H} \end{bmatrix}^\mathbf{H}$, has a closed form solution:

$$\widehat{\mathbf{L}}_j = \begin{cases} \mathbf{L}_j & \text{if } \|\mathbf{L}_j\|_F \leq \sqrt{\frac{\mu r \sigma}{n}} \\ \frac{1}{\|\mathbf{L}_j\|_F} \mathbf{L}_j \cdot \sqrt{\frac{\mu r \sigma}{n}} & \text{otherwise} \end{cases}$$

for $0 \leq j \leq n_1 - 1$ and

$$e_k^\mathbf{T} \widehat{\mathbf{R}} = \begin{cases} e_k^\mathbf{T} \mathbf{R} & \text{if } \|e_k^\mathbf{T} \mathbf{R}\|_2 \leq \sqrt{\frac{\mu r \sigma}{n}} \\ \frac{e_k^\mathbf{T} \mathbf{R}}{\|e_k^\mathbf{T} \mathbf{R}\|_2} \cdot \sqrt{\frac{\mu r \sigma}{n}} & \text{otherwise} \end{cases}$$

for $0 \leq k \leq n_2 - 1$. Let \mathbf{M}_t be the current estimator. The algorithm updates \mathbf{M}_t along gradient descent direction $-\nabla f(\mathbf{M}_t)$ with step size η , followed by projection onto the set \mathcal{M} . The gradient of $f(\mathbf{M})$ is computed with respect to Wirtinger calculus given by $\nabla f = [\nabla_{\mathbf{L}}^{\text{H}} f \quad \nabla_{\mathbf{R}}^{\text{H}} f]^{\text{H}}$ where

$$\begin{aligned}\nabla_{\mathbf{L}} f &= (\mathcal{G}\mathcal{A}^*(\mathcal{A}\mathcal{G}^*(\mathbf{L}\mathbf{R}^{\text{H}}) - \mathbf{D}\mathbf{y})) \mathbf{R} + ((\mathcal{I} - \mathcal{G}\mathcal{G}^*)(\mathbf{L}\mathbf{R}^{\text{H}})) \mathbf{R} + \frac{1}{4}\mathbf{L}(\mathbf{L}^{\text{H}}\mathbf{L} - \mathbf{R}^{\text{H}}\mathbf{R}), \\ \nabla_{\mathbf{R}} f &= (\mathcal{G}\mathcal{A}^*(\mathcal{A}\mathcal{G}^*(\mathbf{L}\mathbf{R}^{\text{H}}) - \mathbf{D}\mathbf{y}))^{\text{H}} \mathbf{L} + ((\mathcal{I} - \mathcal{G}\mathcal{G}^*)(\mathbf{L}\mathbf{R}^{\text{H}}))^{\text{H}} \mathbf{L} + \frac{1}{4}\mathbf{R}(\mathbf{R}^{\text{H}}\mathbf{R} - \mathbf{L}^{\text{H}}\mathbf{L}).\end{aligned}$$

Indeed PGD–VHL algorithm can be efficiently implemented. To obtain the computational cost of ∇f , we first introduce some notations. Let \mathcal{H}_v be the Hankel operator which maps a vector $\mathbf{x} \in \mathbb{C}^n$ into an $n_1 \times n_2$ matrix,

$$\mathcal{H}_v(\mathbf{x}) = \begin{bmatrix} x_0 & \cdots & x_{n_2-1} \\ \vdots & \ddots & \vdots \\ x_{n_1-1} & \cdots & x_{n_1-1} \end{bmatrix},$$

where x_i is the i -th entry of \mathbf{x} . The adjoint of \mathcal{H}_v , denoted by \mathcal{H}_v^* , is a linear mapping from $n_1 \times n_2$ to n . It can be seen that $\mathcal{H}_v^*(\mathbf{L}_v\mathbf{R}_v^{\text{H}})$ can be computed via r fast convolutions by noting that

$$\begin{aligned}[\mathcal{H}_v^*(\mathbf{L}_v\mathbf{R}_v^{\text{H}})]_i &= \left[\mathcal{H}_v^* \left(\sum_{s=1}^r \mathbf{L}_v[:, s] \overline{\mathbf{R}_v[:, s]}^{\text{T}} \right) \right]_i \\ &= \sum_{s=1}^r [\mathcal{H}_v^*(\mathbf{L}_v[:, s] \overline{\mathbf{R}_v[:, s]}^{\text{T}})]_i \\ &= \sum_{s=1}^r (\mathbf{L}_v[:, s] * \overline{\mathbf{R}_v[:, s]})[i],\end{aligned}$$

where $\mathbf{L}_v \in \mathbb{C}^{n_1 \times r}$ and $\mathbf{R}_v \in \mathbb{C}^{n_2 \times r}$. In addition, we can compute $(\mathcal{H}_v(\mathbf{x}))\mathbf{R}_v$ by r fast Hankel matrix–vector multiplications, that is,

$$\begin{aligned}(\mathcal{H}_v(\mathbf{x})\mathbf{R}_v)[j, s] &= \sum_{k=0}^{n_2-1} \mathbf{x}[j+k]\mathbf{R}_v[k, s] \\ &= \sum_{k=0}^{n_2-1} \tilde{\mathbf{x}}[n-1-j-k]\mathbf{R}_v[k, s] \\ &= (\tilde{\mathbf{x}} * \mathbf{R}_v[:, s])[n-1-j],\end{aligned}$$

where $\tilde{\mathbf{x}}$ is a vector reversing the order of \mathbf{x} . Therefore the computational complexity of both $\mathcal{H}_v^*(\mathbf{L}_v\mathbf{R}_v^{\text{H}})$ and $(\mathcal{H}_v(\mathbf{x}))\mathbf{R}_v$ is $\mathcal{O}(rn \log n)$ flops. Moreover, the authors in [12] show that $\mathcal{H}(\mathbf{X}) = \mathbf{P}\tilde{\mathcal{H}}(\mathbf{X})$, where $\tilde{\mathcal{H}}(\mathbf{X})$ is a matrix constructed by stacking all $\{\mathcal{H}_v(\mathbf{e}_\ell^{\text{T}}\mathbf{X})\}_{\ell=1}^s$ on top of one another, and \mathbf{P} is a permutation matrix. Therefore we can compute $\mathcal{G}^*(\mathbf{L}\mathbf{R}^{\text{H}})$ and $\mathcal{G}\mathcal{D}(\mathbf{X})\mathbf{R}$ by using $\mathcal{O}(srn \log n)$ flops. Thus the implementation of our algorithm is very efficient and the main computational complexity in each step is $\mathcal{O}(sr^2n + srn \log n)$.

4 Main result

In this section, we provide a theoretical analysis of PGD–VHL under a random subspace model.

Assumption 4.1. *The column vectors $\{\mathbf{b}_i\}_{i=0}^{n-1}$ of \mathbf{B}^{H} are independently and identically drawn from a distribution F which satisfies the following conditions:*

$$\mathbb{E}[\mathbf{b}_i\mathbf{b}_i^{\text{H}}] = \mathbf{I}_s, \quad i = 0, \dots, n-1, \quad (4.1)$$

$$\max_{0 \leq \ell \leq s-1} |\mathbf{b}_i[\ell]|^2 \leq \mu_0, \quad i = 0, \dots, n-1. \quad (4.2)$$

Remark 4.1. Assumption 4.1 is a standard assumption in RIPless compressed sensing [10] and blind super-resolution [15, 37, 21, 30, 12]. It implies the spectral flatness over point spread functions, which is satisfied in OFDM signals [2] and noisy radar waveforms [26]. Assumption 4.1 holds with $\mu_0 = 1$ by many common random ensembles, for instance, when the components of \mathbf{b} are Rademacher random variables taking the values ± 1 with equal probability or when \mathbf{b} is uniformly sampled from the rows of a Discrete Fourier Transform (DFT) matrix.

Now we present the main result, whose proofs are deferred to Section 6.

Theorem 4.1. Let $\mu \geq \mu_1$ and $\sigma = \sigma_1(\widehat{\Sigma}_0)/(1 - \varepsilon)$ for $0 \leq \varepsilon \leq 1/3$. Let $\eta \leq \frac{\sigma_r}{9000(\mu_0\mu sr\sigma_1)^2}$, $\beta = \frac{\sigma_r}{72}$, and $\mathbf{M}^\natural = \begin{bmatrix} \mathbf{L}^{\natural\text{H}} & \mathbf{R}^{\natural\text{H}} \end{bmatrix}^{\text{H}}$. Suppose \mathbf{X}^\natural obeys the Assumption 2.1 and the subspace \mathbf{B} satisfies the Assumption 4.1. If

$$n \geq c_0 \varepsilon^{-2} \mu_0^2 \mu s^2 r^2 \kappa^2 \log^2(sn),$$

with probability at least $1 - c_1(sn)^{-c_2}$, the sequence $\{\mathbf{M}_t\}$ returned by Algorithm 1 satisfies

$$\text{dist}^2(\mathbf{M}_t, \mathbf{M}^\natural) \leq (1 - \eta\beta)^t \cdot \frac{\varepsilon^2 \sigma_r}{\mu_0 s}, \quad (4.3)$$

where c_0, c_1, c_2 are absolute constants, $\sigma_1 = \sigma_1(\mathbf{Z}^\natural)$, $\sigma_r = \sigma_r(\mathbf{Z}^\natural)$, κ is the condition number of \mathbf{Z}^\natural , and the distance $\text{dist}(\mathbf{M}, \mathbf{M}^\natural)$ is defined as

$$\text{dist}(\mathbf{M}, \mathbf{M}^\natural) = \min_{\mathbf{Q}\mathbf{Q}^{\text{H}} = \mathbf{Q}^{\text{H}}\mathbf{Q} = \mathbf{I}_r} \|\mathbf{M} - \mathbf{M}^\natural\mathbf{Q}\|_{\text{F}}.$$

Remark 4.2. It is worth noting that our results require slightly milder assumptions than that in [12]. The theoretical performance in [12] is established based on an additional assumption, which requires a lower bound of ℓ_2 norm of the row vector of \mathbf{B} . However, the performance guarantee of PGD-VHL is independent of this assumption.

Remark 4.3. Compared with the sample complexity established in [12] for the nuclear norm minimization method, which is $n \geq c\mu_0\mu_1 \cdot sr \log^4(sn)$, Theorem 4.1 implies that PGD-VHL is sub-optimal in terms of s and r . The extra r factor is caused by the technical derivation. Since the convergence is established based on the Frobenius norm and the Frobenius norm of the initial error is bounded by its spectral norm. Details can be found in Section 6.1. The extra s factor is introduced to ensure the initial error to be sufficiently small, i.e., on the order of $1/(\mu_0 s)$, which helps to derive the linear convergence rate of PGD-VHL. We admit that it is an artifact of our proof because subsequent numerical experiments indicate that there approximately exists a linear relationship between n and s or n and r .

Remark 4.4. Theorem 4.1 implies that PGD-VHL converges to \mathbf{M}^\natural with a linear rate. Therefore, after $T = \mathcal{O}((\mu_0\mu sr\kappa)^2 \log(1/\varepsilon))$ iterations, we have $\text{dist}^2(\mathbf{M}_T, \mathbf{M}^\natural) \leq \varepsilon \cdot \text{dist}^2(\mathbf{M}_0, \mathbf{M}^\natural)$. Given the iterates \mathbf{M}_T returned by PGD-VHL, we can estimate \mathbf{X}_T by $\mathcal{D}^{-1}\mathcal{G}^*(\mathbf{L}_T\mathbf{R}_T^{\text{H}})$.

Remark 4.5. As already mentioned, once the data matrix \mathbf{X}^\natural is recovered, the locations $\{\tau_k\}_{k=1}^r$ can be computed from it by spatial smoothing MUSIC algorithm [18, 17, 39, 12] and the weights $\{d_k, \mathbf{h}_k\}_{k=1}^r$ can be estimated by solving an overdetermined linear system [12].

Remark 4.6. Though we have mainly focused on the one-dimensional (1D) blind super-resolution problem, the model and analysis are also applicable for higher dimensional case. Due to space limitations, we omit the theoretical results but provide numerical simulations for two-dimensional (2D) blind super-resolution problem in Section V.B.

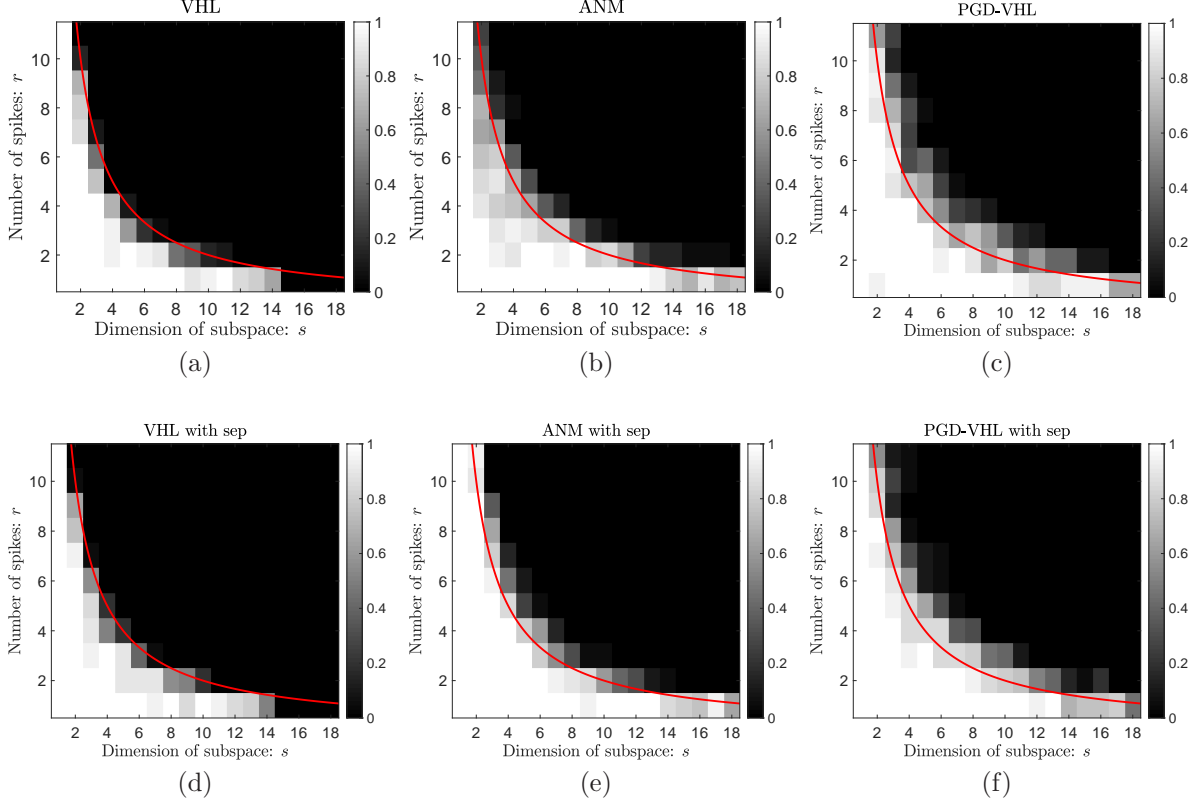


Figure 1: The phase transitions of VHL, ANM and PGD-VHL when $n = 64$. Top: frequencies are randomly generated; Bottom: frequencies obey the separation condition $\Delta := \min_{k \neq j} |\tau_k - \tau_j| \geq 1/n$. The red curve plots the hyperbola curve $rs = 20$.

5 Numerical simulations

In this section, a series of numerical results are provided to illustrate the performance of PGD-VHL. We conduct simulations on 1D signals and 2D signals separately. Moreover, we implement our algorithm with 2D MUSIC [3, 41] to solve the joint delay-Doppler estimation problem, which is an important issue arising in orthogonal frequency-division multiplexing (OFDM) signals. The numerical simulations are executed from MATLAB R2021b on a macOS machine with multi-core Intel CPU at 2.3 GHz CPU and 16 GB RAM. Our code is available at “<https://github.com/jcchen2017/PGDVHL>”.

5.1 Simulation for 1D Signals

We begin by providing the numerical results for 1D signals. The data matrix $\mathbf{X}^\dagger \in \mathbb{C}^{s \times n}$ is generated by $\sum_{k=1}^r d_k \mathbf{h}_k \mathbf{a}_{\tau_k}^\top$. Here the locations $\{\tau_k\}_{k=1}^r$ of the point sources are randomly generated from $[0, 1)$, the coefficients $\{\mathbf{h}_k\}_{k=1}^r$ are i.i.d. sampled from standard Gaussian with normalization, and the amplitudes $\{d_k\}_{k=1}^r$ are selected to be $d_k = (1 + 10^{c_k})e^{-\iota\phi_k}$, where c_k is uniformly sampled from $[0, 1]$ and ϕ_k is uniformly sampled from $[0, 2\pi)$. Moreover, the columns of \mathbf{B} are uniformly sampled from the DFT matrix. The stepsize of PGD-VHL is chosen via backtracking line search.

The first experiment studies the recovery ability of PGD-VHL through the framework of phase transition and we compare it with two convex recovery methods: VHL [12] and ANM [37]. Both VHL and ANM are solved by CVX [19]. PGD-VHL will be terminated if $\|y - \mathcal{A}(\mathbf{X}_t)\|_2 \leq 10^{-5}$ or a maximum number of

iterations is reached. The tests are conducted with $n = 64$ and the varied s and r . We repeat 20 random trials and record the probability of successful recovery in our tests. A trial is declared to be successful if $\|\mathbf{X}_t - \mathbf{X}^\dagger\|_F / \|\mathbf{X}^\dagger\|_F \leq 10^{-3}$. Figure 1(a), 1(b) and 1(c) show the phase transitions of VHL, ANM and PGD-VHL when the locations of point sources are randomly generated, and Figure 1(d), 1(e) and 1(f) illustrate the phase transitions of VHL, ANM and PGD-VHL when the separation condition $\Delta := \min_{j \neq k} |\tau_j - \tau_k| \geq 1/n$ is imposed. In this figure, white color means successful recovery while black color indicates failure. It is interesting to observe that PGD-VHL has a higher phase transition curve than VHL whether the separation condition is satisfied or not. Moreover, by comparing Figure 1(b) with (c), we observe that PGD-VHL is less sensitive to the separation condition than ANM.

In the second experiment, we study the phase transition of PGD-VHL when one of r and s is fixed. Note that in this test, the separation condition is not imposed for PGD-VHL. Figure 2(a) indicates an approximately linear relationship between s and n for the successful recovery when the number of point sources is fixed to be $r = 4$. The same linear relationship between r and n can be observed when the dimension of the subspace is fixed to be $s = 4$, see Figure 2(b). Therefore there exists a gap between our theory and empirical observation and we leave it as future work.

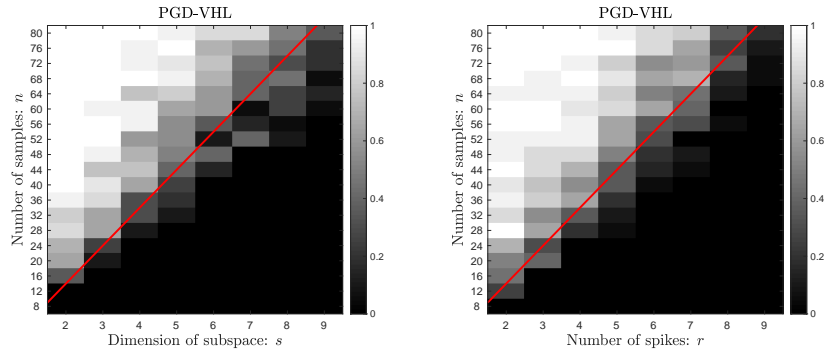


Figure 2: (a) The phase transition of PGD-VHL for varying n and s when $r = 4$. The red line plots the straight line $n = 2.5s$. (b) The phase transition of PGD-VHL for varying n and r when $s = 4$. The red line plots the straight line $n = 2.5r$.

In the third simulation, we investigate the convergence rate of PGD-VHL for $n = 1024$ with fixed s or r . The results are shown in Figure 3. The y -axis denotes $\log(\|\mathbf{X}_t - \mathbf{X}^\dagger\|_F / \|\mathbf{X}^\dagger\|_F)$ and the x -axis represents the iteration number. It can be clearly seen that PGD-VHL converges linearly as shown in our main theorem. Also it is worth pointing out that PGD-VHL can be implemented in high dimensional regimes, where we take $n = 1024$.

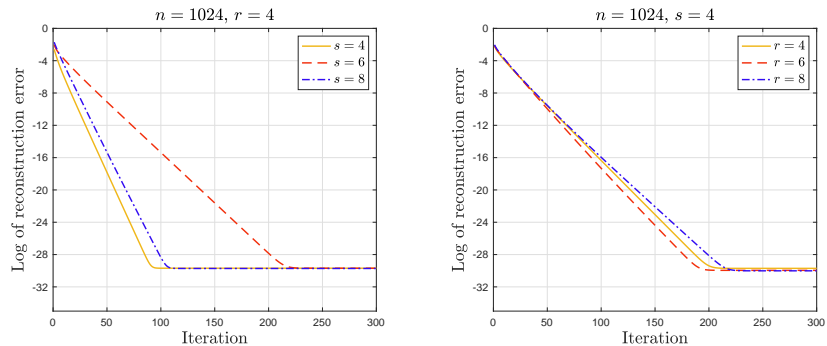


Figure 3: (a) Convergence of PGD-VHL for varying $s = 4, 6, 8$ when $n = 1024$ and $r = 4$. (b) Convergence of PGD-VHL for varying $r = 4, 6, 8$ when $n = 1024$ and $s = 4$.

In the fourth simulation, we conduct the tests to demonstrate the robustness of PGD-VHL to additive noise. More specifically, we collect the measurements corrupted by the noise vector $\mathbf{e} = \sigma_e \cdot \|\mathbf{y}\|_2 \cdot \mathbf{w} / \|\mathbf{w}\|_2$, where \mathbf{y} is the uncontaminated observations, \mathbf{w} is the standard Gaussian vector with i.i.d. entries and σ_e denotes the noise level. In the tests, the noise level σ_e is taken from 10^{-3} to 1, corresponding to the signal-to-noise ratio (SNR) from 60 to 0 dB. For each σ_e , 10 random trials are conducted with $s = r = 4$. As for the number of measurements, we choose $n = 64$ and $n = 128$ for comparison. PGD-VHL is set to be terminated when $\|\mathbf{X}^{t+1} - \mathbf{X}^t\|_F / \|\mathbf{X}^t\|_F \leq 10^{-7}$. In Figure 4, the average relative reconstruction error is plotted with SNR. It can be clearly seen that the relationship between the relative reconstruction error and the noise level is linear for PGD-VHL. Moreover, the relative reconstruction error decreases with the increase of the number of measurements.

We finally compare the running time for ANM, VHL and PGD-VHL when the number of measurements is varied, the number of spikes r is fixed to be 3 and the dimension of subspace s is also fixed to be 3. Note that both VHL and ANM are solved by SDPT3 [32] based on CVX [19]. We repeat 10 random trials for each test. The average computational time for each tested algorithms are shown in Table I. The symbol “-” indicates that the algorithm was terminated due to the lack of memory. It can be seen that PGD-VHL significantly improve the running time compared with ANM and VHL when n is large.

Table 1: Running time comparison for 1D signals when $s = r = 3$.

Methods	$n = 64$	$n = 128$	$n = 256$	$n = 512$
ANM	1.6278s	7.2992s	67.6007s	-
VHL	62.2369s	748.3695s	-	-
PGD-VHL	1.3254s	4.4417s	19.3004s	57.4518s

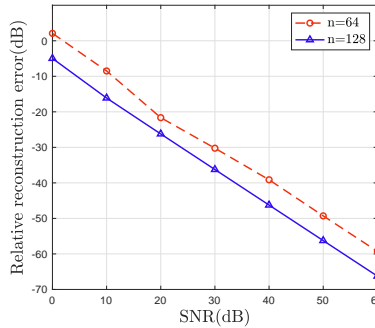


Figure 4: Performance of PGD-VHL under different noise levels

5.2 Simulation for 2D Signals

In this part, we evaluate the performance of our algorithm for 2D signals. The data matrix is given by $\mathbf{X}^{\natural} = \sum_{k=1}^r d_k \mathbf{h}_k (\mathbf{a}_{\tau_{2k}} \otimes \mathbf{a}_{\tau_{1k}})^{\top} \in \mathbb{C}^{s \times n_1 n_2}$ and the samples are generated by

$$\mathbf{y}[j] = \langle \mathbf{b}_j \mathbf{e}_j^{\top}, \mathbf{X}^{\natural} \rangle, \quad j = 0, \dots, n_1 n_2 - 1. \quad (5.1)$$

Here the two dimensional locations $\boldsymbol{\tau}_k := (\tau_{1k}, \tau_{2k})$ are uniformly sampled from $[0, 1) \times [0, 1)$, the amplitudes $\{d_k\}_{k=1}^r$, the coefficients $\{\mathbf{h}_k\}_{k=1}^r$ and the subspace columns $\{\mathbf{b}_j\}_{j=0}^{n_1 n_2 - 1}$ are generated by the same way as the 1D case. Let $\mathbf{X}_{\ell}^{\natural} = \sum_{k=1}^r d_k e^{-2i\pi\tau_{2k}\cdot\ell} (\mathbf{h}_k \mathbf{a}_{\tau_{1k}}^{\top})$ be an $s \times n_1$ matrix, where $\ell = 0, \dots, n_2 - 1$. Let $\mathcal{H}(\mathbf{X}^{\natural})$

be the two-fold vectorized Hankel matrix of \mathbf{X}^{\natural} defined as follows:

$$\mathcal{H}(\mathbf{X}^{\natural}) = \begin{bmatrix} \mathcal{H}(\mathbf{X}_0^{\natural}) & \cdots & \mathcal{H}(\mathbf{X}_{K_2-1}^{\natural}) \\ \vdots & \ddots & \vdots \\ \mathcal{H}(\mathbf{X}_{K_1-1}^{\natural}) & \cdots & \mathcal{H}(\mathbf{X}_{n_2}^{\natural}) \end{bmatrix} \in \mathbb{C}^{sL_1K_1 \times L_2K_2},$$

where $\mathcal{H}(\mathbf{X}_\ell^{\natural}) \in \mathbb{C}^{sL_1 \times L_2}$ is the vectorized Hankel matrix defined in (1.1). Here $L_1 + L_2 = n_1 + 1$ and $K_1 + K_2 = n_2 + 1$. It has been shown in [12] that $\mathcal{H}(\mathbf{X}^{\natural})$ is a rank- r matrix. Therefore, we can naturally generalize our algorithm to the 2D case, and then use the two-dimensional PGD-VHL (PGD-VHL (2D)) to recover \mathbf{X}^{\natural} from (5.1). The phase transition is shown in Figure 5 and the convergence rate of PGD-VHL (2D) for different n_1 and n_2 is shown in Figure 6. Overall, the performance of PGD-VHL (2D) exhibits a similar phenomenon to the 1D case.

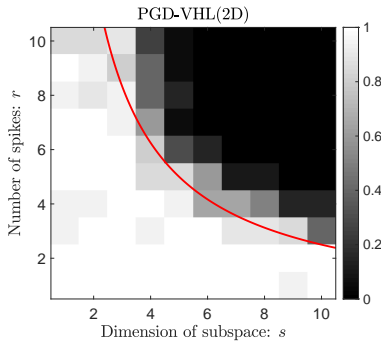


Figure 5: The phase transition of PGD-VHL (2D) for varying s and r when $n_1 = 13$ and $n_2 = 9$. The locations are randomly generated. The red line plots the straight line $sr = 25$.

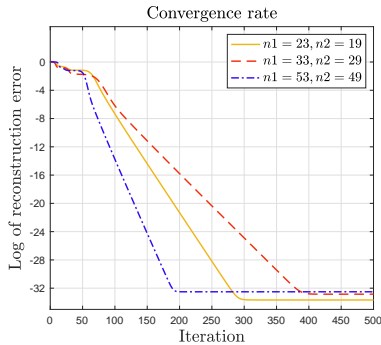


Figure 6: Convergence of PGD-VHL (2D) for 2D signals with $(n_1, n_2) \in \{(23, 19), (33, 29), (53, 49)\}$. Here we fix $s = 3$ and $r = 3$.

5.3 Simulation for joint delay-Doppler estimation from OFDM signals

Furthermore, we evaluate the performance of PGD-VHL (2D) for the problem of joint delay-Doppler estimation from OFDM signals. In this problem, the transmitted signal is divided into M blocks and N orthogonal subcarriers are used in each block. Then the received samples in the n -th subcarrier and m -th block can be formulated as [41]

$$\mathbf{y}_m[n] = \sum_{k=1}^r d_k e^{-2i\pi(n \cdot \Delta f \tau_k + m \cdot \bar{T} f_k)} \mathbf{g}_m[n], \quad (5.2)$$

where r is the number of propagation paths for communication channel, $\{\tau_k, f_k\}_{k=1}^r$ are the delays and Doppler frequencies, $\{d_k\}_{k=1}^r \subset \mathbb{C}$ denote the channel coefficients, Δf is the frequency spacing of adjacent subcarriers, \bar{T} is the duration of each transmission block with $\bar{T}f_k \ll 1$ as stated in [41], and $\{\mathbf{g}_m[n]\}_{n=0, \dots, N-1}$ denote data symbols in the m -th block. For sake of simplicity, we define $\phi_k = \Delta f \tau_k \in [0, 1)$, $\psi_k = \bar{T}f_k \in [0, 1)$. Concatenating $\mathbf{y}_m[n]$ in the vector $\mathbf{y}_m \in \mathbb{C}^N$ and stacking \mathbf{y}_m yield that

$$\mathbf{y} = \left(\sum_{k=0}^r d_k \mathbf{a}_{\psi_k} \otimes \mathbf{a}_{\phi_k} \right) \odot \mathbf{g} \in \mathbb{C}^{MN},$$

where $\mathbf{g} = [\mathbf{g}_1 \ \dots \ \mathbf{g}_M]^\top \in \mathbb{C}^{MN}$ and $\mathbf{g}_m = [\mathbf{g}_m[0] \ \dots \ \mathbf{g}_m[N-1]]^\top \in \mathbb{C}^N$. As pointed in [2, 35], since the waveforms in OFDM have a flat spectrum, \mathbf{g} can be approximately represented as $\mathbf{g} = \mathbf{B}\mathbf{h}$, where \mathbf{B} should obey the isotropy and incoherence properties in Assumption 4.1. Then the received samples can be rewritten as

$$\mathbf{y}[j] = \left\langle \mathbf{b}_j \mathbf{e}_j^\top, \sum_{k=1}^r d_k \mathbf{h}(\mathbf{a}_{\psi_k} \otimes \mathbf{a}_{\phi_k})^\top \right\rangle \quad (5.3)$$

for $j = 0, \dots, MN - 1$. It can be seen that (5.3) is a special case of (5.1) where \mathbf{h} is independent to the two dimensional locations $\{(\psi_k, \phi_k)\}_{k=1}^r$.

In our numerical simulation, We set $N = 13, M = 9$ and $s = r = 4$. Each row of \mathbf{B} is generated from the following distribution described in [15, 35], i.e.,

$$\mathbf{b}_k = [1 \quad e^{2\pi i f_k} \quad \dots \quad e^{2\pi i (s-1) f_k}]^\top$$

for $k = 0, \dots, MN - 1$, where f_k is chosen uniformly at random in $[0, 1]$. The locations $\{(\psi_k, \phi_k)\}_{k=1}^r$ are chosen uniformly at random from $[0, 1) \times [0, 1)$, and the coefficient vector \mathbf{h} is generated from standard Gaussian with normalization. The data matrix $\sum_{k=1}^r d_k \mathbf{h}(\mathbf{a}_{\psi_k} \otimes \mathbf{a}_{\phi_k})^\top$ can be firstly recovered via PGD-VHL (2D), then the locations $\{(\psi_k, \phi_k)\}_{k=1}^r$ are retrieved by 2D MUSIC and the channel coefficients $\{d_k\}_{k=1}^r$ are estimated by solving an overdetermined linear system [12]. The results are presented in Figure 7. It is shown that implementing PGD-VHL (2D) with 2D MUSIC can exactly recover delays and Doppler frequencies.

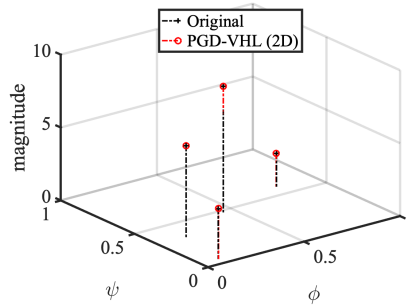


Figure 7: Performance of PGD-VHL (2D) for joint delay-Doppler estimation problem.

6 Proof of Theorem 4.1

The proof follows a well established route that has been widely used in non-convex optimization for low rank matrix recovery [9, 42, 5]. In a nutshell, the initialization provided in Algorithm 1 will be shown to lie in a basin of attraction where the sequence returned by Algorithm 1 converges linearly to the true solution. Despite this, the proof details are quite involved and substantially different. We first list two useful lemmas, whose proofs are deferred to Section 6.1 and 6.2.

Lemma 6.1. Suppose \mathbf{Z}^\natural is μ_1 -incoherent and $n \geq c_0 \varepsilon^{-2} \kappa^2 \mu_0^2 \mu s^2 r^2 \log^2(sn)$. Then one has

$$\text{dist}^2(\mathbf{M}_0, \mathbf{M}^\natural) \leq \frac{\varepsilon^2 \sigma_r}{\mu_0 s}$$

with probability at least $1 - (sn)^{-c_1}$.

Lemma 6.2. Let $\{\mathbf{M}_t\}$ be the sequence returned by Algorithm 1. Denote $\mathbf{\Delta}_t := \mathbf{M}_t - \mathbf{M}^\natural \mathbf{Q}_t$, where

$$\mathbf{Q}_t = \arg \min_{\mathbf{Q} \mathbf{Q}^\mathbf{H} = \mathbf{Q}^\mathbf{H} \mathbf{Q} = \mathbf{I}_r} \|\mathbf{M}_t - \mathbf{M}^\natural \mathbf{Q}\|_{\text{F}}.$$

Let $\eta \leq \frac{\sigma_r}{9000(\mu_0 \mu s r \sigma_1)^2}$, $\beta = \frac{\sigma_r}{72}$. Then with probability $1 - (sn)^{-c}$, one has

$$\text{dist}^2(\mathbf{M}_t, \mathbf{M}^\natural) \leq (1 - \eta \beta)^t \text{dist}^2(\mathbf{M}_0, \mathbf{M}^\natural)$$

for $t = 1, 2, \dots$.

Combining Lemma 6.1 and Lemma 6.2 together, we complete the proof.

6.1 Proof of Lemma 6.1

We begin our presentation of the proof with a useful lemma whose proof is provided in Section 6.3.

Lemma 6.3. Suppose that \mathbf{Z}^\natural is μ_1 -incoherent. Then with probability at least $1 - (sn)^{-c_1}$, the matrix $\widehat{\mathbf{Z}}_0 = \mathcal{P}_r(\mathcal{GDA}^*(\mathbf{y}))$ obeys

$$\|\widehat{\mathbf{Z}}_0 - \mathbf{Z}^\natural\| \leq c_0 \sigma_1 \sqrt{\frac{\mu_0 \mu_1 s r \log^2(sn)}{n}}, \quad (6.1)$$

where c_0 and c_1 are absolute constants.

By Lemma 6.3 and the assumption that n should be larger than $c_0 \varepsilon^{-2} \kappa^2 \mu_0^2 \mu s^2 r^2 \log^2(sn)$, the event

$$\|\widehat{\mathbf{Z}}_0 - \mathbf{Z}^\natural\| \leq c_1 \sqrt{\frac{\mu_0 \mu_1 s r \log^2(sn)}{n}} \sigma_1(\mathbf{Z}^\natural) \leq \varepsilon \sigma_1(\mathbf{Z}^\natural)$$

occurs with probability at least $1 - (sn)^{-c_1}$, which implies that

$$\sigma_1(\mathbf{Z}^\natural) \leq \frac{\sigma_1(\widehat{\mathbf{Z}}_0)}{1 - \varepsilon} =: \sigma \text{ and } \sigma_1(\widehat{\mathbf{Z}}_0) \leq (1 + \varepsilon) \sigma \leq 2\sigma.$$

By the definition of \mathcal{M} in (2.10), it can be seen that $\mathbf{M}^\natural \widehat{\mathbf{Q}}_0 \in \mathcal{M}$, where $\widehat{\mathbf{Q}}_0 = \arg \min_{\mathbf{Q}} \|\widehat{\mathbf{M}}_0 - \mathbf{M}^\natural \mathbf{Q}\|_{\text{F}}$.

Thus we have

$$\begin{aligned} \text{dist}(\mathbf{M}_0, \mathbf{M}^\natural) &= \min_{\mathbf{Q}} \|\mathbf{M}_0 - \mathbf{M}^\natural \mathbf{Q}\|_{\text{F}} \\ &\leq \|\mathbf{M}_0 - \mathbf{M}^\natural \widehat{\mathbf{Q}}_0\|_{\text{F}} \\ &= \|\mathcal{P}_{\mathcal{M}}(\widehat{\mathbf{M}}_0 - \mathbf{M}^\natural \widehat{\mathbf{Q}}_0)\|_{\text{F}} \\ &\leq \|\widehat{\mathbf{M}}_0 - \mathbf{M}^\natural \widehat{\mathbf{Q}}_0\|_{\text{F}} \\ &= \text{dist}(\widehat{\mathbf{M}}_0, \mathbf{M}^\natural). \end{aligned} \quad (6.2)$$

To complete the proof, it suffices to control $\text{dist}(\widehat{\mathbf{M}}_0, \mathbf{M}^\natural)$. A straightforward computation yields that

$$\begin{aligned}
\text{dist}^2(\widehat{\mathbf{M}}_0, \mathbf{M}^\natural) &\stackrel{(a)}{\leq} \frac{1}{2(\sqrt{2}-1)\sigma_r^2(\mathbf{M}^\natural)} \left\| \widehat{\mathbf{M}}_0 \widehat{\mathbf{M}}_0^H - \mathbf{M}^\natural \mathbf{M}^{\natural H} \right\|_F^2 \\
&\stackrel{(b)}{\leq} \frac{1}{4(\sqrt{2}-1)\sigma_r} \left\| \widehat{\mathbf{M}}_0 \widehat{\mathbf{M}}_0^H - \mathbf{M}^\natural \mathbf{M}^{\natural H} \right\|_F^2 \\
&\stackrel{(c)}{\leq} \frac{1}{4(\sqrt{2}-1)\sigma_r} \cdot 4 \left\| \widehat{\mathbf{Z}}_0 - \mathbf{Z}^\natural \right\|_F^2 \\
&\leq \frac{1}{(\sqrt{2}-1)\sigma_r} \cdot 2r \left\| \widehat{\mathbf{Z}}_0 - \mathbf{Z}^\natural \right\|_F^2 \\
&\leq \frac{2r}{(\sqrt{2}-1)\sigma_r} \cdot \frac{\mu_0 \mu s r \log^2(sn)}{n} \sigma_1^2 \\
&\leq \frac{\varepsilon^2 \sigma_r}{\mu_0 s}
\end{aligned}$$

provided that $n \geq c_0 \varepsilon^{-2} \kappa^2 \mu_0^2 \mu s^2 r^2 \log^2(sn)$, where step (a) is due to Lemma 5.4 in [34], step (b) has used the fact $\sigma_r(\mathbf{M}^\natural) = \sqrt{2}\sigma_r$, and the step (c) can be derived as follows.

Let $\mathbf{A}_1, \mathbf{B}_1 \in \mathbb{C}^{s n_1 \times r}$ and $\mathbf{A}_2, \mathbf{B}_2 \in \mathbb{C}^{n_2 \times r}$ be four complex matrices. It is direct to obtain that

$$\begin{aligned}
\langle \mathbf{A}_1 \mathbf{A}_1^H, \mathbf{B}_1 \mathbf{B}_1^H \rangle + \langle \mathbf{A}_2 \mathbf{A}_2^H, \mathbf{B}_2 \mathbf{B}_2^H \rangle &= \langle \mathbf{A}_1^H \mathbf{B}_1, \mathbf{A}_1^H \mathbf{B}_1 \rangle + \langle \mathbf{A}_2^H \mathbf{B}_2, \mathbf{A}_2^H \mathbf{B}_2 \rangle \\
&\geq 2\Re(\langle \mathbf{A}_1 \mathbf{A}_2^H, \mathbf{B}_1 \mathbf{B}_2^H \rangle).
\end{aligned} \tag{6.3}$$

Then a simple calculation yields that

$$\left\| \widehat{\mathbf{M}}_0 \widehat{\mathbf{M}}_0^H - \mathbf{M}^\natural \mathbf{M}^{\natural H} \right\|_F^2 = 2 \left\| \widehat{\mathbf{U}}_0 \widehat{\mathbf{\Sigma}}_0 \widehat{\mathbf{V}}_0^H - \mathbf{U} \mathbf{\Sigma} \mathbf{V}^H \right\|_F^2 + \left\| \widehat{\mathbf{U}}_0 \widehat{\mathbf{\Sigma}}_0 \widehat{\mathbf{U}}_0^H - \mathbf{U} \mathbf{\Sigma} \mathbf{U}^H \right\|_F^2 + \left\| \widehat{\mathbf{V}}_0 \widehat{\mathbf{\Sigma}}_0 \widehat{\mathbf{V}}_0^H - \mathbf{V} \mathbf{\Sigma} \mathbf{V}^H \right\|_F^2.$$

Denote $\mathbf{A}_1 = \widehat{\mathbf{U}}_0 \widehat{\mathbf{\Sigma}}_0^{1/2}$, $\mathbf{B}_1 = \mathbf{U} \mathbf{\Sigma}^{1/2}$, $\mathbf{A}_2 = \widehat{\mathbf{V}}_0 \widehat{\mathbf{\Sigma}}_0^{1/2}$ and $\mathbf{B}_2 = \mathbf{V} \mathbf{\Sigma}^{1/2}$. Applying (6.3) can be easily verified that

$$\left\| \widehat{\mathbf{U}}_0 \widehat{\mathbf{\Sigma}}_0 \widehat{\mathbf{U}}_0^H - \mathbf{U} \mathbf{\Sigma} \mathbf{U}^H \right\|_F^2 + \left\| \widehat{\mathbf{V}}_0 \widehat{\mathbf{\Sigma}}_0 \widehat{\mathbf{V}}_0^H - \mathbf{V} \mathbf{\Sigma} \mathbf{V}^H \right\|_F^2 \leq 2 \left\| \widehat{\mathbf{U}}_0 \widehat{\mathbf{\Sigma}}_0 \widehat{\mathbf{V}}_0^H - \mathbf{U} \mathbf{\Sigma} \mathbf{V}^H \right\|_F^2.$$

Hence

$$\begin{aligned}
\left\| \widehat{\mathbf{M}}_0 \widehat{\mathbf{M}}_0^H - \mathbf{M}^\natural \mathbf{M}^{\natural H} \right\|_F^2 &\leq 4 \left\| \widehat{\mathbf{U}}_0 \widehat{\mathbf{\Sigma}}_0 \widehat{\mathbf{V}}_0^H - \mathbf{U} \mathbf{\Sigma} \mathbf{V}^H \right\|_F^2 \\
&= 4 \left\| \widehat{\mathbf{Z}}_0 - \mathbf{Z}^\natural \right\|_F^2.
\end{aligned}$$

Thus we complete the proof of Lemma 6.1.

6.2 Proof of Lemma 6.2

We first establish a regularity condition in the following lemma whose proof is provided in Section 6.4.

Lemma 6.4. *Let $\mathbf{\Delta} = \mathbf{M} - \mathbf{M}^\natural \mathbf{Q}$, where $\mathbf{Q} = \arg \min_{\mathbf{Q} \mathbf{Q}^H = \mathbf{Q}^\natural \mathbf{Q}^\natural H} \left\| \mathbf{M} - \mathbf{M}^\natural \mathbf{Q} \right\|_F$. Then one has*

$$\Re(\langle \nabla f(\mathbf{M}), \mathbf{\Delta} \rangle) \geq \frac{\eta}{2} \left\| \nabla f(\mathbf{M}) \right\|_F^2 + \frac{\beta}{2} \left\| \mathbf{\Delta} \right\|_F^2 \tag{6.4}$$

happens with high probability for all \mathbf{M} such that $\left\| \mathbf{\Delta} \right\|_F^2 \leq \frac{\varepsilon^2 \sigma_r}{\mu_0 s}$, where $\eta \leq \frac{\sigma_r}{9000(\mu_0 \mu s r \sigma_1)^2}$, and $\beta = \frac{\sigma_r}{72}$.

Let $\widehat{\mathbf{M}}_{t+1} = \mathbf{M}_t - \eta \nabla f(\mathbf{M}_t)$. Under the condition of (6.4), one has

$$\begin{aligned}
\text{dist}^2(\mathbf{M}_{t+1}, \mathbf{M}^\natural) &\stackrel{(a)}{\leq} \text{dist}^2(\widehat{\mathbf{M}}_{t+1}, \mathbf{M}^\natural) \\
&\leq \left\| \widehat{\mathbf{M}}_{t+1} - \mathbf{M}^\natural \mathbf{Q}_t \right\|_{\text{F}}^2 \\
&= \left\| \boldsymbol{\Delta}_t - \eta \nabla f(\mathbf{M}_t) \right\|_{\text{F}}^2 \\
&= \left\| \boldsymbol{\Delta}_t \right\|_{\text{F}}^2 + \eta^2 \left\| \nabla f(\mathbf{M}_t) \right\|_{\text{F}}^2 - 2\eta \Re \left(\langle \boldsymbol{\Delta}_t, \nabla f(\mathbf{M}_t) \rangle \right) \\
&\stackrel{(b)}{\leq} \left\| \boldsymbol{\Delta}_t \right\|_{\text{F}}^2 + \eta^2 \left\| \nabla f(\mathbf{M}_t) \right\|_{\text{F}}^2 - \eta^2 \left\| \nabla f(\mathbf{M}_t) \right\|_{\text{F}}^2 - \beta \eta \left\| \boldsymbol{\Delta}_t \right\|_{\text{F}}^2 \\
&= (1 - \eta\beta) \left\| \boldsymbol{\Delta}_t \right\|_{\text{F}}^2,
\end{aligned}$$

where step (a) follows the same argument as (6.2) and step (b) is due to (6.4). Then a little algebra yields that

$$\begin{aligned}
\text{dist}^2(\mathbf{M}_{t+1}, \mathbf{M}^\natural) &\leq (1 - \eta\beta)^{t+1} \text{dist}^2(\mathbf{M}_0, \mathbf{M}^\natural) \\
&\leq (1 - \eta\beta)^{t+1} \frac{\varepsilon^2 \sigma_r}{\mu_0 s},
\end{aligned}$$

which completes the proof of Lemma 6.2.

6.3 Proof of Lemma 6.3

Notice that $\mathcal{GDA}^*(\mathbf{y}) = \mathcal{GA}^* \mathbf{D}(\mathbf{y}) = \mathcal{GA}^* \mathcal{AG}^*(\mathbf{Z}^\natural)$. A simple computation yields that

$$\begin{aligned}
\mathbb{E} [\mathcal{GA}^* \mathcal{AG}^*(\mathbf{Z}^\natural)] &= \mathbb{E} \left[\mathcal{G} \left(\sum_{i=0}^{n-1} \langle \mathbf{b}_i \mathbf{e}_i^\top, \mathcal{G}^*(\mathbf{Z}^\natural) \rangle \mathbf{b}_i \mathbf{e}_i^\top \right) \right] \\
&= \mathcal{G} \left(\sum_{i=0}^{n-1} \mathbb{E} [\mathbf{b}_i \mathbf{b}_i^\text{H} \mathcal{G}^*(\mathbf{Z}^\natural) \mathbf{e}_i \mathbf{e}_i^\top] \right) \\
&= \mathcal{GG}^*(\mathbf{Z}^\natural) = \mathbf{Z}^\natural,
\end{aligned}$$

where the third equality is due to the isotropy property of $\{\mathbf{b}_i\}_{i=0}^{n-1}$. Let us first bound

$$\left\| \mathcal{GA}^* \mathcal{AG}^*(\mathbf{Z}^\natural) - \mathbb{E} [\mathcal{GA}^* \mathcal{AG}^*(\mathbf{Z}^\natural)] \right\|$$

by the matrix Bernstein inequality (6.29). The matrix $\mathcal{GA}^* \mathcal{AG}^*(\mathbf{Z}^\natural) - \mathbb{E} [\mathcal{GA}^* \mathcal{AG}^*(\mathbf{Z}^\natural)]$ can be rewritten as

$$\begin{aligned}
\mathcal{GA}^* \mathcal{AG}^*(\mathbf{Z}^\natural) - \mathbb{E} [\mathcal{GA}^* \mathcal{AG}^*(\mathbf{Z}^\natural)] &= \sum_{i=0}^{n-1} \mathcal{G} \left((\mathbf{b}_i \mathbf{b}_i^\text{H} - \mathbf{I}_s) \mathcal{G}^*(\mathbf{Z}^\natural) \mathbf{e}_i \mathbf{e}_i^\top \right) \\
&= \sum_{i=0}^{n-1} \mathbf{G}_i \otimes \left((\mathbf{b}_i \mathbf{b}_i^\text{H} - \mathbf{I}_s) \mathcal{G}^*(\mathbf{Z}^\natural) \mathbf{e}_i \right) \\
&=: \sum_{i=0}^{n-1} \mathbf{Y}_i.
\end{aligned}$$

Notice that $\{\mathbf{Y}_i\}_{i=0}^{n-1}$ are independent mean-zero random matrices with

$$\begin{aligned}
\|\mathbf{Y}_i\| &= \left\| \mathbf{G}_i \otimes \left((\mathbf{b}_i \mathbf{b}_i^\text{H} - \mathbf{I}_s) \mathcal{G}^*(\mathbf{Z}^\natural) \mathbf{e}_i \right) \right\| \\
&\leq \|\mathbf{G}_i\| \cdot \left\| (\mathbf{b}_i \mathbf{b}_i^\text{H} - \mathbf{I}_s) \mathcal{G}^*(\mathbf{Z}^\natural) \mathbf{e}_i \right\|
\end{aligned}$$

$$\begin{aligned}
&\leq \frac{1}{\sqrt{\omega_i}} \cdot \max\{\|\mathbf{b}_i\|_2^2, 1\} \cdot \|\mathcal{G}^*(\mathbf{Z}^\natural)\mathbf{e}_i\|_2 \\
&\stackrel{(a)}{\leq} s\mu_0 \cdot \max_i \frac{1}{\sqrt{\omega_i}} \|\mathcal{G}^*(\mathbf{Z}^\natural)\mathbf{e}_i\|_2 \\
&\stackrel{(b)}{\leq} s\mu_0 \cdot \frac{\mu_1 r}{n} \sigma_1,
\end{aligned}$$

where step (a) follows from (4.2) and step (b) is due to Lemma 6.6. Moreover, letting $\mathbf{w}_i := (\mathbf{b}_i \mathbf{b}_i^\mathbf{H} - \mathbf{I}_s) \mathcal{G}^*(\mathbf{Z}^\natural) \mathbf{e}_i$, we have

$$\begin{aligned}
\left\| \mathbb{E} \left[\sum_{i=0}^{n-1} \mathbf{Y}_i^\mathbf{H} \mathbf{Y}_i \right] \right\| &= \left\| \sum_{i=0}^{n-1} \mathbb{E} [(\mathbf{G}_i \otimes \mathbf{w}_i)^\mathbf{H} (\mathbf{G}_i \otimes \mathbf{w}_i)] \right\| \\
&= \left\| \sum_{i=0}^{n-1} (\mathbf{G}_i^\mathbf{H} \mathbf{G}_i) \cdot \mathbb{E} [\|\mathbf{w}_i\|_2^2] \right\| \\
&\leq \sum_{i=0}^{n-1} \|\mathbf{G}_i^\mathbf{H} \mathbf{G}_i\| \cdot \mathbb{E} [\|\mathbf{w}_i\|_2^2] \\
&\stackrel{(a)}{\leq} \sum_{i=0}^{n-1} \frac{1}{\omega_i} \cdot s\mu_0 \|\mathcal{G}^*(\mathbf{Z}^\natural)\mathbf{e}_i\|_2^2 \\
&\stackrel{(b)}{\leq} s\mu_0 \cdot \sqrt{\frac{\mu_1 r \log(sn)}{n}} \sigma_1,
\end{aligned}$$

where step (a) follows from $\|\mathbf{G}_i\| \leq 1/\sqrt{\omega_i}$ and the fact $\mathbb{E} [\|\mathbf{w}_i\|_2^2] \leq s\mu_0 \cdot \|\mathcal{G}^*(\mathbf{Z}^\natural)\mathbf{e}_i\|_2^2$, and step (b) is due to Lemma 6.6. Moreover, the fact used in step (a) can be proved as follows:

$$\begin{aligned}
\mathbb{E} [\|\mathbf{w}_i\|_2^2] &= \mathbb{E} \left[\mathbf{e}_i^\mathbf{T} (\mathcal{G}^*(\mathbf{Z}^\natural))^\mathbf{H} (\mathbf{b}_i \mathbf{b}_i^\mathbf{H} - \mathbf{I}_s)^2 \mathcal{G}^*(\mathbf{Z}^\natural) \mathbf{e}_i \right] \\
&= \mathbf{e}_i^\mathbf{T} (\mathcal{G}^*(\mathbf{Z}^\natural))^\mathbf{H} \mathbb{E} [(\mathbf{b}_i \mathbf{b}_i^\mathbf{H} - \mathbf{I}_s)^2] \mathcal{G}^*(\mathbf{Z}^\natural) \mathbf{e}_i \\
&= \mathbf{e}_i^\mathbf{T} (\mathcal{G}^*(\mathbf{Z}^\natural))^\mathbf{H} \mathbb{E} [\|\mathbf{b}_i\|_2^2 \mathbf{b}_i \mathbf{b}_i^\mathbf{H} - \mathbf{I}_s] \mathcal{G}^*(\mathbf{Z}^\natural) \mathbf{e}_i \\
&\leq (\mu_0 s - 1) \cdot \|\mathcal{G}^*(\mathbf{Z}^\natural)\mathbf{e}_i\|_2^2 \\
&\leq \mu_0 s \|\mathcal{G}^*(\mathbf{Z}^\natural)\mathbf{e}_i\|_2^2,
\end{aligned}$$

where the third line is due to (4.1). Similarly, one has

$$\begin{aligned}
\left\| \mathbb{E} \left[\sum_{i=0}^{n-1} \mathbf{Y}_i \mathbf{Y}_i^\mathbf{H} \right] \right\| &\leq \sum_{i=0}^{n-1} \|\mathbf{G}_i\|^2 \cdot \|\mathbb{E} [\mathbf{w}_i \mathbf{w}_i^\mathbf{H}]\| \\
&\leq \sum_{i=0}^{n-1} \|\mathbf{G}_i\|^2 \cdot \mathbb{E} [\|\mathbf{w}_i\|_2^2] \\
&\leq s\mu_0 \cdot \sqrt{\frac{\mu_1 r \log(sn)}{n}} \sigma_1.
\end{aligned}$$

Applying the matrix Bernstein inequality (6.29) shows that, with probability greater than $1 - (sn)^{-c_1}$,

$$\|\mathcal{G} \mathcal{A}^* \mathcal{A} \mathcal{G}^*(\mathbf{Z}^\natural) - \mathbb{E} [\mathcal{G} \mathcal{A}^* \mathcal{A} \mathcal{G}^*(\mathbf{Z}^\natural)]\| \leq c_1 \sqrt{s\mu_0 \log(sn)} \cdot \sqrt{\frac{\mu_1 r \log(sn)}{n}} \sigma_1 + c_2 s\mu_0 \log(sn) \cdot \frac{\mu_1 r}{n} \sigma_1$$

$$\leq c_3 \sqrt{\frac{\mu_0 \mu_1 s r \log^2(sn)}{n}} \sigma_1$$

provided $n \geq c_0 \mu_0 \mu_1 s r \log^2(sn)$. Therefore, the event

$$\begin{aligned} \left\| \widehat{\mathbf{Z}}_0 - \mathbf{Z}^\natural \right\| &= \left\| \mathcal{P}_r (\mathcal{G} \mathcal{A} \mathcal{A}^* \mathcal{G}^* (\mathbf{Z}^\natural)) - \mathbf{Z}^\natural \right\| \\ &\leq \left\| \mathcal{P}_r (\mathcal{G} \mathcal{A} \mathcal{A}^* \mathcal{G}^* (\mathbf{Z}^\natural)) - \mathcal{G} \mathcal{A}^* \mathcal{A} \mathcal{G}^* (\mathbf{Z}^\natural) \right\| \\ &\quad + \left\| \mathcal{G} \mathcal{A}^* \mathcal{A} \mathcal{G}^* (\mathbf{Z}^\natural) - \mathbf{Z}^\natural \right\| \\ &\leq 2 \left\| \mathcal{G} \mathcal{A}^* \mathcal{A} \mathcal{G}^* (\mathbf{Z}^\natural) - \mathbf{Z}^\natural \right\| \\ &\leq c_0 \sqrt{\frac{\mu_0 \mu_1 s r \log^2(sn)}{n}} \sigma_1. \end{aligned}$$

occurs with probability at least $1 - (sn)^{-c_1}$. Finally we complete the proof.

6.4 Proof of Lemma 6.4

The proof includes two parts. We will show that

$$\Re(\langle \nabla f(\mathbf{M}), \mathbf{\Delta} \rangle) \geq \frac{1}{72} \sigma_r \|\mathbf{\Delta}\|_{\mathbb{F}}^2 + \frac{1}{8} \left\| \mathbf{M}^{\natural \text{H}} \mathbf{S} \mathbf{\Delta} \right\|_{\mathbb{F}}^2 \quad (6.5)$$

and

$$\|\nabla f(\mathbf{M})\|_{\mathbb{F}}^2 \leq 125 (\mu_0 \mu_1 s r \sigma_1)^2 \|\mathbf{\Delta}\|_{\mathbb{F}}^2 + \frac{1}{2} \sigma_1 \left\| \mathbf{M}^{\natural \text{H}} \mathbf{S} \mathbf{\Delta} \right\|_{\mathbb{F}}^2 \quad (6.6)$$

provided $\varepsilon \leq \frac{1}{3}$. By the assumption

$$\eta \leq \frac{\sigma_r}{9000 (\mu_0 \mu_1 s r \sigma_1)^2} \leq \frac{1}{2\sigma_1} \text{ and } \beta = \frac{\sigma_r}{72},$$

we have

$$\begin{aligned} \frac{\eta}{2} \|\nabla f(\mathbf{M})\|_{\mathbb{F}}^2 + \frac{\beta}{2} \|\mathbf{\Delta}\|_{\mathbb{F}}^2 &\leq \left(\frac{1}{2} \frac{\sigma_r}{9000 (\mu_0 \mu_1 s r \sigma_1)^2} \cdot 125 (\mu_0 \mu_1 s r \sigma_1)^2 + \frac{1}{2} \frac{\sigma_r}{72} \right) \|\mathbf{\Delta}\|_{\mathbb{F}}^2 + \frac{1}{2} \cdot \frac{1}{2\sigma_1} \cdot \frac{1}{2} \sigma_1 \left\| \mathbf{M}^{\natural \text{H}} \mathbf{S} \mathbf{\Delta} \right\|_{\mathbb{F}}^2 \\ &\leq \frac{\sigma_r}{72} \|\mathbf{\Delta}\|_{\mathbb{F}}^2 + \frac{1}{8} \left\| \mathbf{M}^{\natural \text{H}} \mathbf{S} \mathbf{\Delta} \right\|_{\mathbb{F}}^2 \\ &\leq \Re(\langle \nabla f(\mathbf{M}), \mathbf{\Delta} \rangle). \end{aligned}$$

6.4.1 Proof of (6.5)

Let $\nabla f_1, \nabla f_2$ and ∇f_3 be the matrices given by

$$\begin{aligned} \nabla f_1 &= \begin{bmatrix} (\mathcal{G} \mathcal{A}^* (\mathcal{A} \mathcal{G}^* (\mathbf{L} \mathbf{R}^{\text{H}}) - \mathbf{D} \mathbf{y})) \mathbf{R} \\ (\mathcal{G} \mathcal{A}^* (\mathcal{A} \mathcal{G}^* (\mathbf{L} \mathbf{R}^{\text{H}}) - \mathbf{D} \mathbf{y}))^{\text{H}} \mathbf{L} \end{bmatrix}, \\ \nabla f_2 &= \begin{bmatrix} ((\mathcal{I} - \mathcal{G} \mathcal{G}^*) (\mathbf{L} \mathbf{R}^{\text{H}})) \mathbf{R} \\ ((\mathcal{I} - \mathcal{G} \mathcal{G}^*) (\mathbf{L} \mathbf{R}^{\text{H}}))^{\text{H}} \mathbf{L} \end{bmatrix}, \\ \nabla f_3 &= \frac{1}{4} \begin{bmatrix} \mathbf{L} (\mathbf{L}^{\text{H}} \mathbf{L} - \mathbf{R}^{\text{H}} \mathbf{R}) \\ \mathbf{R} (\mathbf{R}^{\text{H}} \mathbf{R} - \mathbf{L}^{\text{H}} \mathbf{L}) \end{bmatrix}. \end{aligned}$$

A straightforward computation yields that

$$\Re(\langle \nabla f(\mathbf{M}), \mathbf{\Delta} \rangle) = \Re(\langle \nabla f_1, \mathbf{\Delta} \rangle) + \Re(\langle \nabla f_2, \mathbf{\Delta} \rangle) + \Re(\langle \nabla f_3, \mathbf{\Delta} \rangle).$$

We will bound these three terms separately. For the sake of simplification, let $\mathbf{\Delta} = [\mathbf{\Delta}_{\mathbf{L}}^{\text{H}} \quad \mathbf{\Delta}_{\mathbf{R}}^{\text{H}}]^{\text{H}}$ where $\mathbf{\Delta}_{\mathbf{L}} = \mathbf{L} - \mathbf{L}^{\natural} \mathbf{Q} \in \mathbb{C}^{s n_1 \times r}$ and $\mathbf{\Delta}_{\mathbf{R}} = \mathbf{R} - \mathbf{R}^{\natural} \mathbf{Q} \in \mathbb{C}^{n_2 \times r}$.

Bounding $\Re(\langle \nabla f_1, \Delta \rangle)$ By applying $D\mathbf{y} = \mathcal{A}\mathcal{G}^*(\mathbf{Z}^\natural)$, we can rewrite $\Re(\langle \nabla f_1, \Delta \rangle)$ as

$$\Re(\langle \nabla f_1, \Delta \rangle) = \Re\left(\left\langle \mathcal{G}\mathcal{A}^*\mathcal{A}\mathcal{G}^*(L\mathbf{R}^H - L^\natural\mathbf{R}^{\natural H}), \Delta_L\mathbf{R}^H + L\Delta_R^H \right\rangle\right). \quad (6.7)$$

Notice that

$$\begin{aligned} L\mathbf{R}^H - L^\natural\mathbf{R}^{\natural H} &= (\Delta_L + L^\natural Q)(\Delta_R + R^\natural Q)^H - L^\natural\mathbf{R}^{\natural H} \\ &= \underbrace{\Delta_L\Delta_R^H}_{:=\Psi} + \underbrace{\Delta_L(R^\natural Q)^H + (L^\natural Q)\Delta_R^H}_{:=\Phi}. \end{aligned} \quad (6.8)$$

and

$$\begin{aligned} \Delta_L\mathbf{R}^H + L\Delta_R^H &= \Delta_L(\Delta_R + R^\natural Q)^H + (\Delta_L + L^\natural Q)\Delta_R^H \\ &= 2\Delta_L\Delta_R^H + \Delta_L(R^\natural Q)^H + (L^\natural Q)\Delta_R^H \\ &= 2\Psi + \Phi. \end{aligned} \quad (6.9)$$

Then $\Re(\langle \nabla f_1, \Delta \rangle)$ can be bounded as follows:

$$\begin{aligned} \Re(\langle \nabla f_1, \Delta \rangle) &= \Re(\langle \mathcal{A}\mathcal{G}^*(\Phi + \Psi), \mathcal{A}\mathcal{G}^*(\Phi + 2\Psi) \rangle) \\ &= \|\mathcal{A}\mathcal{G}^*(\Phi)\|_2^2 + 2\|\mathcal{A}\mathcal{G}^*(\Psi)\|_2^2 + 3\Re(\langle \mathcal{A}\mathcal{G}^*(\Phi), \mathcal{A}\mathcal{G}^*(\Psi) \rangle) \\ &\geq \|\mathcal{A}\mathcal{G}^*(\Phi)\|_2^2 + 2\|\mathcal{A}\mathcal{G}^*(\Psi)\|_2^2 - 3|\langle \mathcal{A}\mathcal{G}^*(\Phi), \mathcal{A}\mathcal{G}^*(\Psi) \rangle| \\ &\geq \|\mathcal{A}\mathcal{G}^*(\Phi)\|_2^2 + 2\|\mathcal{A}\mathcal{G}^*(\Psi)\|_2^2 - 3\|\mathcal{A}\mathcal{G}^*(\Phi)\|_2 \cdot \|\mathcal{A}\mathcal{G}^*(\Psi)\|_2 \\ &\geq \frac{3}{4}\|\mathcal{A}\mathcal{G}^*(\Phi)\|_2^2 - 7\|\mathcal{A}\mathcal{G}^*(\Psi)\|_2^2 \\ &\geq \frac{3}{4}\|\mathcal{A}\mathcal{G}^*(\Phi)\|_2^2 - \frac{7\varepsilon^2}{4}\sigma_r\|\Delta\|_F^2, \end{aligned} \quad (6.10)$$

where the second line is due to $\langle \mathbf{x}, \mathbf{x} \rangle = \|\mathbf{x}\|_2^2$ and $\Re(\langle \mathbf{x}, \mathbf{y} \rangle) = \Re(\langle \mathbf{y}, \mathbf{x} \rangle)$ for any vectors $\mathbf{x}, \mathbf{y} \in \mathbb{C}^n$, the third line is due to $\Re(\langle \mathbf{x}, \mathbf{y} \rangle) \leq |\langle \mathbf{x}, \mathbf{y} \rangle|$, and the last second line is due to $a + 2b - 3\sqrt{ab} \geq \frac{3}{4}a - 7b$ for any $a, b \geq 0$ and the last line is due to the fact $\|\mathcal{A}\mathcal{G}^*(\Psi)\|_2^2 \leq \frac{\varepsilon^2}{4}\sigma_r\|\Delta\|_F^2$. Moreover the fact used in the last line can be proved as follows:

$$\begin{aligned} \|\mathcal{A}\mathcal{G}^*(\Psi)\|_2^2 &= \|\mathcal{A}\mathcal{G}^*(\Delta_L\Delta_R^H)\|_2^2 \\ &\leq (\|\mathcal{A}\| \|\mathcal{G}^*\| \cdot \|\Delta_L\Delta_R^H\|_F)^2 \\ &\leq \mu_0 s \cdot \frac{1}{4} \left(\|\Delta_L\|_F^2 + \|\Delta_R\|_F^2 \right)^2 \\ &= \frac{\mu_0 s}{4} \|\Delta\|_F^4 \\ &\leq \frac{\varepsilon^2}{4}\sigma_r\|\Delta\|_F^2, \end{aligned} \quad (6.11)$$

where the second line is due to $\|\mathcal{A}\| \leq \sqrt{\mu_0 s}$, $\|\mathcal{G}^*\| \leq 1$ and the last line is due to $\|\Delta\|_F^2 \leq \frac{\varepsilon^2\sigma_r}{\mu_0 s}$. Plugging (6.10) into (6.7) reveals that

$$\Re(\langle \nabla f_1, \Delta \rangle) \geq \frac{3}{4}\|\mathcal{A}\mathcal{G}^*(\Phi)\|_2^2 - \frac{7\varepsilon^2}{4}\sigma_r\|\Delta\|_F^2. \quad (6.12)$$

Bounding $\Re(\langle \nabla f_2, \Delta \rangle)$ This term can be bounded as follows:

$$\Re(\langle \nabla f_2, \Delta \rangle) = \Re(\langle (\mathcal{I} - \mathcal{G}\mathcal{G}^*)(L\mathbf{R}^H), \Delta_L\mathbf{R}^H + L\Delta_R^H \rangle)$$

$$\begin{aligned}
&= \Re \left(\left\langle (\mathcal{I} - \mathcal{G}\mathcal{G}^*)(\mathbf{L}\mathbf{R}^{\mathbf{H}} - \mathbf{L}^{\mathbf{h}}\mathbf{R}^{\mathbf{h}\mathbf{H}}), \Delta_{\mathbf{L}}\mathbf{R}^{\mathbf{H}} + \mathbf{L}\Delta_{\mathbf{R}}^{\mathbf{H}} \right\rangle \right) \\
&= \Re \left(\langle (\mathcal{I} - \mathcal{G}\mathcal{G}^*)(\Phi + \Psi), (\Phi + 2\Psi) \rangle \right) \\
&\geq \|(\mathcal{I} - \mathcal{G}\mathcal{G}^*)(\Phi)\|_{\mathbb{F}}^2 + 2\|(\mathcal{I} - \mathcal{G}\mathcal{G}^*)(\Psi)\|_{\mathbb{F}}^2 \\
&\quad - 3\|(\mathcal{I} - \mathcal{G}\mathcal{G}^*)(\Phi)\|_{\mathbb{F}} \cdot \|(\mathcal{I} - \mathcal{G}\mathcal{G}^*)(\Psi)\|_{\mathbb{F}} \\
&\geq \frac{3}{4}\|(\mathcal{I} - \mathcal{G}\mathcal{G}^*)(\Phi)\|_{\mathbb{F}}^2 - 7\|(\mathcal{I} - \mathcal{G}\mathcal{G}^*)(\Psi)\|_{\mathbb{F}}^2, \tag{6.13}
\end{aligned}$$

where the second line is due to $(\mathcal{I} - \mathcal{G}\mathcal{G}^*)(\mathbf{L}^{\mathbf{h}}\mathbf{R}^{\mathbf{h}\mathbf{H}}) = \mathbf{0}$ and the last line follows from the fact that $a + 2b - 3\sqrt{ab} \geq \frac{3}{4}a - 7b$ for any $a, b \geq 0$. Combining (6.12) and (6.13) together, one has

$$\begin{aligned}
\Re \langle \nabla f_1, \Delta \rangle + \Re \langle \nabla f_2, \Delta \rangle &\geq \frac{3}{4}\|\mathcal{A}\mathcal{G}^*(\Phi)\|_2^2 - \frac{7\varepsilon^2}{4}\sigma_r\|\Delta\|_{\mathbb{F}}^2 + \frac{3}{4}\|(\mathcal{I} - \mathcal{G}\mathcal{G}^*)(\Phi)\|_{\mathbb{F}}^2 - 7\|(\mathcal{I} - \mathcal{G}\mathcal{G}^*)(\Psi)\|_{\mathbb{F}}^2 \\
&\geq \frac{3}{4}\left(\|\mathcal{A}\mathcal{G}^*(\Phi)\|_2^2 + \|(\mathcal{I} - \mathcal{G}\mathcal{G}^*)(\Phi)\|_{\mathbb{F}}^2\right) - \frac{7\varepsilon^2}{4}\sigma_r\|\Delta\|_{\mathbb{F}}^2 - 7\|\Psi\|_{\mathbb{F}}^2, \tag{6.14}
\end{aligned}$$

where the last line follows from the fact that $\mathcal{I} - \mathcal{G}\mathcal{G}^*$ is a projection operator. Let T be the tangent space at $\mathbf{Z}^{\mathbf{h}}$ defined as follows

$$T := \{\mathbf{U}\mathbf{J}^{\mathbf{H}} + \mathbf{K}\mathbf{V}^{\mathbf{H}} : \mathbf{J} \in \mathbb{C}^{n_2 \times r}, \mathbf{K} \in \mathbb{C}^{s n_1 \times r}\}.$$

It can be seen that $\Phi \in T$. Therefore a simple calculation yields that

$$\begin{aligned}
\|\mathcal{A}\mathcal{G}^*(\Phi)\|_2^2 + \|(\mathcal{I} - \mathcal{G}\mathcal{G}^*)(\Phi)\|_{\mathbb{F}}^2 &= \langle \mathcal{A}^*\mathcal{A}\mathcal{G}^*(\Phi), \Phi \rangle + \langle \Phi, \Phi \rangle - \langle \mathcal{G}\mathcal{G}^*(\Phi), \Phi \rangle \\
&\geq \|\Phi\|_{\mathbb{F}}^2 - |\langle \mathcal{G}(\mathcal{I} - \mathcal{A}^*\mathcal{A})\mathcal{G}^*(\Phi), \Phi \rangle| \\
&= \|\Phi\|_{\mathbb{F}}^2 - |\langle \mathcal{P}_T\mathcal{G}(\mathcal{I} - \mathcal{A}^*\mathcal{A})\mathcal{G}^*\mathcal{P}_T(\Phi), \Phi \rangle| \\
&\geq (1 - \varepsilon)\|\Phi\|_{\mathbb{F}}^2, \tag{6.15}
\end{aligned}$$

where the last line follows from Lemma 6.7 and the assumption on n . In addition, we have

$$\begin{aligned}
\|\Psi\|_{\mathbb{F}}^2 &\leq (\|\Delta_{\mathbf{L}}\|_{\mathbb{F}}\|\Delta_{\mathbf{R}}\|_{\mathbb{F}})^2 \\
&\leq \frac{1}{4}\|\Delta\|_{\mathbb{F}}^4 \\
&\leq \frac{\varepsilon^2\sigma_r}{4}\|\Delta\|_{\mathbb{F}}^2, \tag{6.16}
\end{aligned}$$

where we use $\|\Delta\|_{\mathbb{F}}^2 \leq \frac{\varepsilon^2\sigma_r(\mathbf{Z}^{\mathbf{h}})}{s\mu_0} \leq \varepsilon^2\sigma_r(\mathbf{Z}^{\mathbf{h}})$. Hence plugging (6.15) and (6.16) into (6.14) yields that

$$\begin{aligned}
\Re \langle \nabla f_1, \Delta \rangle + \Re \langle \nabla f_2, \Delta \rangle &\geq \frac{3}{4}(1 - \varepsilon)\|\Phi\|_{\mathbb{F}}^2 - \frac{7\varepsilon^2}{2}\sigma_r\|\Delta\|_{\mathbb{F}}^2 \\
&\geq \frac{1}{2}\|\Phi\|_{\mathbb{F}}^2 - \frac{7\varepsilon^2}{2}\sigma_r\|\Delta\|_{\mathbb{F}}^2 \\
&= \frac{1}{2}\left(\|\Delta_{\mathbf{L}}(\mathbf{R}^{\mathbf{h}}\mathbf{Q})^{\mathbf{H}}\|_{\mathbb{F}}^2 + \|\mathbf{L}^{\mathbf{h}}\mathbf{Q}\Delta_{\mathbf{R}}^{\mathbf{H}}\|_{\mathbb{F}}^2\right) - \frac{7\varepsilon^2}{2}\sigma_r\|\Delta\|_{\mathbb{F}}^2 \\
&\quad + \Re \left(\langle \Delta_{\mathbf{L}}(\mathbf{R}^{\mathbf{h}}\mathbf{Q})^{\mathbf{H}}, (\mathbf{L}^{\mathbf{h}}\mathbf{Q})\Delta_{\mathbf{R}}^{\mathbf{H}} \rangle \right) \\
&\geq \left(\frac{1}{2} - \frac{7\varepsilon^2}{2} \right) \sigma_r \|\Delta\|_{\mathbb{F}}^2 + \Re \left(\langle \Delta_{\mathbf{L}}^{\mathbf{H}}(\mathbf{L}^{\mathbf{h}}\mathbf{Q}), (\mathbf{R}^{\mathbf{h}}\mathbf{Q})^{\mathbf{H}}\Delta_{\mathbf{R}} \rangle \right) \\
&\geq \frac{1}{9}\sigma_r\|\Delta\|_{\mathbb{F}}^2 + \Re \left(\langle \Delta_{\mathbf{L}}^{\mathbf{H}}(\mathbf{L}^{\mathbf{h}}\mathbf{Q}), (\mathbf{R}^{\mathbf{h}}\mathbf{Q})^{\mathbf{H}}\Delta_{\mathbf{R}} \rangle \right), \tag{6.17}
\end{aligned}$$

where the last line is due to $\varepsilon \leq \frac{1}{3}$.

Bounding $\Re(\langle \nabla f_3, \Delta \rangle)$ Denote

$$S = \begin{bmatrix} I_{sn_1} & \\ & -I_{n_2} \end{bmatrix}.$$

We can bound $\Re(\langle \nabla f_3, \Delta \rangle)$ as follows:

$$\begin{aligned}
4\Re(\langle \nabla f_3, \Delta \rangle) &= \Re(\langle SMM^H SM, \Delta \rangle) \\
&= \Re(\langle M^H SM, M^H S \Delta \rangle) \\
&= \Re(\langle (\Delta + M^\natural Q)^H S(\Delta + M^\natural Q), (\Delta + M^\natural Q)^H S \Delta \rangle) \\
&= \|\Delta^H S \Delta\|_F^2 + \|(M^\natural Q)^H S \Delta\|_F^2 + 3\Re(\langle (M^\natural Q)^H S \Delta, \Delta^H S \Delta \rangle) + \Re(\langle (M^\natural Q)^H S \Delta, \Delta^H S(M^\natural Q) \rangle) \\
&= \frac{1}{2} \|(M^\natural Q)^H S \Delta\|_F^2 + \frac{1}{2} \|(M^\natural Q)^H S \Delta + 3\Delta^H S \Delta\|_F^2 - \frac{7}{2} \|\Delta^H S \Delta\|_F^2 + \Re(\langle (M^\natural Q)^H S \Delta, \Delta^H S(M^\natural Q) \rangle) \\
&= \frac{1}{2} \|(M^\natural Q)^H S \Delta\|_F^2 + \frac{1}{2} \|(M^\natural Q)^H S \Delta + 3\Delta^H S \Delta\|_F^2 - \frac{7}{2} \|\Delta^H S \Delta\|_F^2 \\
&\quad + \Re(\langle (M^\natural Q)^H \Delta, \Delta^H (M^\natural Q) \rangle) - 4\Re(\langle \Delta_L^H (L^\natural Q), (R^\natural Q)^H \Delta_R \rangle) \\
&\geq \frac{1}{2} \|(M^\natural Q)^H S \Delta\|_F^2 - \frac{7}{2} \|\Delta^H S \Delta\|_F^2 - 4\Re(\langle \Delta_L^H (L^\natural Q), (R^\natural Q)^H \Delta_R \rangle). \tag{6.18}
\end{aligned}$$

The fourth equality is due to $(M^\natural Q)^H S(M^\natural Q) = \mathbf{0}$. The last equality follows from

$$\begin{aligned}
\Re(\langle \Delta_L^H (L^\natural Q), (R^\natural Q)^H \Delta_R \rangle) &= \Re(\langle (R^\natural Q)^H \Delta_R, \Delta_L^H (L^\natural Q) \rangle) \\
&= \Re(\langle (L^\natural Q)^H \Delta_L, \Delta_R^H (R^\natural Q) \rangle).
\end{aligned}$$

Finally, combining (6.18) with (6.17) yields that

$$\begin{aligned}
\Re(\langle \nabla f(M), \Delta \rangle) &\geq \frac{1}{9} \sigma_r \|\Delta\|_F^2 + \frac{1}{8} \left\| M^{\natural H} S \Delta \right\|_F^2 - \frac{7}{8} \|\Delta^H S \Delta\|_F^2 \\
&\geq \frac{1}{72} \sigma_r \|\Delta\|_F^2 + \frac{1}{8} \left\| M^{\natural H} S \Delta \right\|_F^2, \tag{6.19}
\end{aligned}$$

where the last line follows from that $\|\Delta^H S \Delta\|_F^2 \leq \|\Delta\|_F^4 \leq \frac{\varepsilon^2 \sigma_r}{\mu_0 s} \|\Delta\|_F^2$ and $\varepsilon \leq \frac{1}{3}$.

6.4.2 Proof of (6.6)

Applying simple triangular inequality yields that

$$\begin{aligned}
\|\nabla f(M)\|_F^2 &= \|\nabla f_1 + \nabla f_2 + \nabla f_3\|_F^2 \\
&\leq 2\|\nabla f_1 + \nabla f_2\|_F^2 + 2\|\nabla f_3\|_F^2 \\
&\leq 4\|\nabla f_1\|_F^2 + 4\|\nabla f_2\|_F^2 + 2\|\nabla f_3\|_F^2. \tag{6.20}
\end{aligned}$$

We will bound these three terms separately.

Bounding $\|\nabla f_1\|_F^2$ For any

$$X = \begin{bmatrix} X_L^H & X_R^H \end{bmatrix}^H \in \mathbb{C}^{(sn_1+n_2) \times r}$$

such that $\|X\|_F = 1$, we have

$$\begin{aligned}
|\langle \nabla f_1, X \rangle|^2 &= |\langle \mathcal{G}A^*(\mathcal{A}\mathcal{G}^*(LR^H) - Dy), X_L R^H + L X_R^H \rangle|^2 \\
&= \left| \langle \mathcal{G}A^* \mathcal{A}\mathcal{G}^*(LR^H - L^\natural R^{\natural H}), X_L R^H + L X_R^H \rangle \right|^2
\end{aligned}$$

$$\begin{aligned}
&\leq (|\langle \mathcal{G}\mathcal{A}^* \mathcal{A}\mathcal{G}^*(\mathbf{L}\Delta_R^H), \mathbf{X}_L \mathbf{R}^H \rangle| \\
&\quad + |\langle \mathcal{G}\mathcal{A}^* \mathcal{A}\mathcal{G}^*(\Delta_L(\mathbf{R}^\natural \mathbf{Q})^H), \mathbf{X}_L \mathbf{R}^H \rangle| \\
&\quad + |\langle \mathcal{G}\mathcal{A}^* \mathcal{A}\mathcal{G}^*(\mathbf{L}\Delta_R^H), \mathbf{L}\mathbf{X}_L^H \rangle| \\
&\quad + |\langle \mathcal{G}\mathcal{A}^* \mathcal{A}\mathcal{G}^*(\Delta_L(\mathbf{R}^\natural \mathbf{Q})^H), \mathbf{L}\mathbf{X}_L^H \rangle|)^2.
\end{aligned} \tag{6.21}$$

where we have used the fact $\mathbf{L}\mathbf{R}^H - \mathbf{L}^\natural \mathbf{R}^{\natural H} = \mathbf{L}\Delta_R^H + \Delta_L(\mathbf{R}^\natural \mathbf{Q})^H$. Apparently, the upper bounds of the above four terms can be established similarly. We focus on the first term $|\langle \mathcal{G}\mathcal{A}^* \mathcal{A}\mathcal{G}^*(\mathbf{L}\Delta_R^H), \mathbf{X}_L \mathbf{R}^H \rangle|$ and its upper bound can be obtained as follows:

$$\begin{aligned}
|\langle \mathcal{G}\mathcal{A}^* \mathcal{A}\mathcal{G}^*(\mathbf{L}\Delta_R^H), \mathbf{X}_L \mathbf{R}^H \rangle| &= |\langle \mathcal{A}\mathcal{G}^*(\mathbf{L}\Delta_R^H), \mathcal{A}\mathcal{G}^*(\mathbf{X}_L \mathbf{R}^H) \rangle| \\
&\leq \sum_{i=0}^{n-1} |\langle \mathbf{b}_i \mathbf{e}_i^\top, \mathcal{G}^*(\mathbf{L}\Delta_R^H) \rangle| \cdot |\langle \mathbf{b}_i \mathbf{e}_i^\top, \mathcal{G}^*(\mathbf{X}_L \mathbf{R}^H) \rangle| \\
&= \sum_{i=0}^{n-1} |\langle \mathcal{G}(\mathbf{b}_i \mathbf{e}_i^\top), \mathbf{L}\Delta_R^H \rangle| \cdot |\langle \mathcal{G}(\mathbf{b}_i \mathbf{e}_i^\top), \mathbf{X}_L \mathbf{R}^H \rangle| \\
&= \sum_{i=0}^{n-1} |\langle \mathbf{G}_i \otimes \mathbf{b}_i, \mathbf{L}\Delta_R^H \rangle| \cdot |\langle \mathbf{G}_i \otimes \mathbf{b}_i, \mathbf{X}_L \mathbf{R}^H \rangle|.
\end{aligned} \tag{6.22}$$

To complete the proof, it suffers to control $|\langle \mathbf{G}_i \otimes \mathbf{b}_i, \mathbf{L}\Delta_R^H \rangle|$ and $|\langle \mathbf{G}_i \otimes \mathbf{b}_i, \mathbf{X}_L \mathbf{R}^H \rangle|$. Notice that

$$\begin{aligned}
|\langle \mathbf{G}_i \otimes \mathbf{b}_i, \mathbf{L}\Delta_R^H \rangle| &= \left| \frac{1}{\sqrt{w_i}} \sum_{j+k=i} \langle (\mathbf{e}_j \otimes \mathbf{b}_i) \mathbf{e}_k^\top, \mathbf{L}\Delta_R^H \rangle \right| \\
&\leq \frac{1}{\sqrt{w_i}} \sum_{j+k=i} \|(\mathbf{e}_j^\top \otimes \mathbf{b}_i^H) \mathbf{L}\|_2 \| \mathbf{e}_k^\top \Delta_R \|_2 \\
&\leq \sqrt{\sum_{j+k=i} \|(\mathbf{e}_j^\top \otimes \mathbf{b}_i^H) \mathbf{L}\|_2^2 \| \mathbf{e}_k^\top \Delta_R \|_2^2} \\
&= \sqrt{\sum_{j+k=i} \|\mathbf{b}_i^H \mathbf{L}_j\|_2^2 \| \mathbf{e}_k^\top \Delta_R \|_2^2} \\
&\leq \sqrt{\sum_{j+k=i} \|\mathbf{b}_i\|_2^2 \|\mathbf{L}_j\|_F^2 \| \mathbf{e}_k^\top \Delta_R \|_2^2} \\
&\leq \sqrt{\mu_0 s} \cdot \sqrt{\sum_{j+k=i} \|\mathbf{L}_j\|_F^2 \| \mathbf{e}_k^\top \Delta_R \|_2^2} \\
&\leq \sqrt{\mu_0 s} \cdot \sqrt{\frac{\mu r \sigma}{n}} \cdot \sqrt{\sum_{j+k=i} \| \mathbf{e}_k^\top \Delta_R \|_2^2}.
\end{aligned} \tag{6.23}$$

Similarly one has

$$\begin{aligned}
|\langle \mathbf{G}_i \otimes \mathbf{b}_i, \mathbf{X}_L \mathbf{R}^H \rangle| &\leq \sqrt{\mu_0 s} \cdot \sqrt{\sum_{j+k=i} \|[\mathbf{X}_L]_j\|_F^2 \| \mathbf{e}_k^\top \mathbf{R} \|_2^2} \\
&\leq \sqrt{\mu_0 s} \cdot \sqrt{\frac{\mu r \sigma}{n}} \cdot \sqrt{\sum_{j+k=i} \|[\mathbf{X}_L]_j\|_F^2}.
\end{aligned} \tag{6.24}$$

Plugging (6.23) and (6.24) into (6.22) yields that

$$\begin{aligned} |\langle \mathcal{G}\mathcal{A}^* \mathcal{A}\mathcal{G}^*(\mathbf{L}\Delta_R^H), \mathbf{X}_L \mathbf{R}^H \rangle| &\leq \frac{\mu_0 s \cdot \mu r \sigma}{n} \sum_{i=0}^{n-1} \sqrt{\sum_{j+k=i} \|\mathbf{e}_k^\top \Delta_R\|_2^2} \cdot \sqrt{\sum_{j+k=i} \|[\mathbf{X}_L]_j\|_F^2} \\ &\leq \mu_0 s \cdot \mu r \sigma \cdot \|\Delta_R\|_F \cdot \|\mathbf{X}_L\|_F. \end{aligned}$$

Using the same argument, one has

$$\begin{aligned} |\langle \mathcal{G}\mathcal{A}^* \mathcal{A}\mathcal{G}^*(\Delta_L(\mathbf{R}^\natural \mathbf{Q})^H), \mathbf{X}_L \mathbf{R}^H \rangle| &\leq \mu_0 s \cdot \mu r \sigma \cdot \|\Delta_L\|_F \cdot \|\mathbf{X}_L\|_F, \\ |\langle \mathcal{G}\mathcal{A}^* \mathcal{A}\mathcal{G}^*(\mathbf{L}\Delta_R^H), \mathbf{L}\mathbf{X}_L^H \rangle| &\leq \mu_0 s \cdot \mu r \sigma \cdot \|\Delta_R\|_F \cdot \|\mathbf{X}_L\|_F, \\ |\langle \mathcal{G}\mathcal{A}^* \mathcal{A}\mathcal{G}^*(\Delta_L(\mathbf{R}^\natural \mathbf{Q})^H), \mathbf{L}\mathbf{X}_R^H \rangle| &\leq \mu_0 s \cdot \mu r \sigma \cdot \|\Delta_L\|_F \cdot \|\mathbf{X}_R\|_F. \end{aligned}$$

Hence we can obtain

$$\begin{aligned} |\langle \nabla f_1, \mathbf{X} \rangle|^2 &\leq (\mu_0 \mu s r \sigma)^2 \cdot (\|\Delta_R\|_F \|\mathbf{X}_L\|_F + \|\Delta_L\|_F \|\mathbf{X}_L\|_F + \|\Delta_R\|_F \|\mathbf{X}_R\|_F + \|\Delta_L\|_F \|\mathbf{X}_R\|_F)^2 \\ &= (\mu_0 \mu s r \sigma)^2 \cdot (\|\Delta_L\|_F + \|\Delta_R\|_F)^2 \cdot (\|\mathbf{X}_L\|_F + \|\mathbf{X}_R\|_F)^2 \\ &\leq 4(\mu_0 \mu s r \sigma)^2 \|\Delta\|_F^2, \end{aligned}$$

where the last line is due to $\|\mathbf{X}\|_F^2 = \|\mathbf{X}_L\|_F^2 + \|\mathbf{X}_R\|_F^2 = 1$. Thus we have

$$\begin{aligned} \|\nabla f_1\|_F^2 &= \sup_{\|\mathbf{X}\|_F=1} |\langle \nabla f_1, \mathbf{X} \rangle|^2 \\ &\leq 4(\mu_0 \mu s r \sigma)^2 \|\Delta\|_F^2. \end{aligned} \tag{6.25}$$

Bounding $\|\nabla f_2\|_F^2$ For any $\mathbf{X} \in \mathbb{C}^{(s n_1 + n_2) \times r}$ such that $\|\mathbf{X}\|_F = 1$, one has

$$\begin{aligned} |\langle \nabla f_2, \mathbf{X} \rangle| &\leq |\langle (\mathcal{I} - \mathcal{G}\mathcal{G}^*)(\mathbf{L}\mathbf{R}^H), \mathbf{X}_L \mathbf{R}^H + \mathbf{L}\mathbf{X}_R^H \rangle| \\ &= \left| \langle (\mathcal{I} - \mathcal{G}\mathcal{G}^*)(\mathbf{L}\mathbf{R}^H - \mathbf{L}^\natural \mathbf{R}^{\natural H}), \mathbf{X}_L \mathbf{R}^H + \mathbf{L}\mathbf{X}_R^H \rangle \right| \\ &\leq \left\| (\mathcal{I} - \mathcal{G}\mathcal{G}^*)(\mathbf{L}\mathbf{R}^H - \mathbf{L}^\natural \mathbf{R}^{\natural H}) \right\|_F \cdot \|\mathbf{X}_L \mathbf{R}^H + \mathbf{L}\mathbf{X}_R^H\|_F \\ &\leq \left\| \mathbf{L}\mathbf{R}^H - \mathbf{L}^\natural \mathbf{R}^{\natural H} \right\|_F \cdot \|\mathbf{X}_L \mathbf{R}^H + \mathbf{L}\mathbf{X}_R^H\|_F. \end{aligned}$$

We bound both terms separately.

- Bounding $\left\| \mathbf{L}\mathbf{R}^H - \mathbf{L}^\natural \mathbf{R}^{\natural H} \right\|_F$. It can be bounded as follows:

$$\begin{aligned} \left\| \mathbf{L}\mathbf{R}^H - \mathbf{L}^\natural \mathbf{R}^{\natural H} \right\|_F &= \left\| \mathbf{L}\Delta_R^H + \Delta_L(\mathbf{R}^\natural \mathbf{Q})^H \right\|_F \\ &\leq \|\mathbf{L}\| \|\Delta_R\|_F + \|\mathbf{R}^\natural\| \|\Delta_L\|_F \\ &\leq (1 + \varepsilon)\sqrt{\sigma_1} \|\Delta_R\|_F + \sqrt{\sigma_1} \|\Delta_L\|_F \\ &\leq (1 + \varepsilon)\sqrt{\sigma_1} \cdot \sqrt{2} \|\Delta\|_F, \end{aligned}$$

where we have used the fact $\|\mathbf{L}\| \leq \|\Delta_L\| + \|\mathbf{L}^\natural\| \leq \|\Delta_L\|_F + \sqrt{\sigma_1} \leq \|\Delta\|_F + \sqrt{\sigma_1} \leq (1 + \varepsilon)\sqrt{\sigma_1}$.

- Bounding $\left\| \mathbf{X}_L \mathbf{R}^H + \mathbf{L}\mathbf{X}_R^H \right\|_F$. It can be bounded as follows:

$$\begin{aligned} \left\| \mathbf{X}_L \mathbf{R}^H + \mathbf{L}\mathbf{X}_R^H \right\|_F &\leq \|\mathbf{R}\| \|\mathbf{X}_L\|_F + \|\mathbf{L}\| \|\mathbf{X}_R\|_F \\ &\leq (1 + \varepsilon)\sqrt{\sigma_1} (\|\mathbf{X}_L\|_F + \|\mathbf{X}_R\|_F) \\ &\leq \sqrt{2}(1 + \varepsilon)\sqrt{\sigma_1}. \end{aligned}$$

Combining together and simple computation yields that

$$\begin{aligned}\|\nabla f_2\|_{\mathbb{F}}^2 &= \sup_{\|\mathbf{X}\|_{\mathbb{F}}=1} |\langle \nabla f_3, \mathbf{X} \rangle|^2 \\ &\leq 4(1+\varepsilon)^4 \sigma_1^2 \cdot \|\Delta\|_{\mathbb{F}}^2.\end{aligned}\tag{6.26}$$

Bounding $\|\nabla f_3\|_{\mathbb{F}}^2$ Recall that

$$\mathbf{S} = \begin{bmatrix} \mathbf{I}_{sn_1} & \\ & -\mathbf{I}_{n_2} \end{bmatrix}.$$

A straightforward computation yields that

$$\begin{aligned}\|\nabla f_3\|_{\mathbb{F}}^2 &= \frac{1}{16} \left(\|\mathbf{L}(\mathbf{L}^H \mathbf{L} - \mathbf{R}^H \mathbf{R})\|_{\mathbb{F}}^2 + \|\mathbf{R}(\mathbf{R}^H \mathbf{R} \mathbf{R}^H \mathbf{R})\|_{\mathbb{F}}^2 \right) \\ &= \frac{1}{16} \|\mathbf{S} \mathbf{M} \mathbf{M}^H \mathbf{S} \mathbf{M}\|_{\mathbb{F}}^2 \\ &= \frac{1}{16} \left\| \mathbf{S} (\mathbf{M} \mathbf{M}^H - \mathbf{M}^{\natural} \mathbf{M}^{\natural H}) \mathbf{S} \mathbf{M} + \mathbf{S} \mathbf{M}^{\natural} \mathbf{M}^{\natural H} \mathbf{S} \mathbf{M} \right\|_{\mathbb{F}}^2 \\ &\leq \frac{1}{8} \left\| \mathbf{S} (\mathbf{M} \mathbf{M}^H - \mathbf{M}^{\natural} \mathbf{M}^{\natural H}) \mathbf{S} \mathbf{M} \right\|_{\mathbb{F}}^2 + \frac{1}{8} \left\| \mathbf{S} \mathbf{M}^{\natural} \mathbf{M}^{\natural H} \mathbf{S} \mathbf{M} \right\|_{\mathbb{F}}^2 \\ &\leq \frac{1}{8} \|\mathbf{M}\|^2 \cdot \left\| \mathbf{M} \mathbf{M}^H - \mathbf{M}^{\natural} \mathbf{M}^{\natural H} \right\|_{\mathbb{F}}^2 + \frac{1}{8} \|\mathbf{M}^{\natural}\|^2 \cdot \left\| \mathbf{M}^{\natural H} \mathbf{S} (\mathbf{M}^{\natural} + \Delta) \right\|_{\mathbb{F}}^2 \\ &\stackrel{(a)}{=} \frac{1}{8} \|\mathbf{M}\|^2 \cdot \left\| \mathbf{M}^{\natural} \Delta^H + \Delta \mathbf{M}^{\natural H} + \Delta \Delta^H \right\|_{\mathbb{F}}^2 + \frac{1}{8} \|\mathbf{M}^{\natural}\|^2 \cdot \left\| \mathbf{M}^{\natural H} \mathbf{S} \Delta \right\|_{\mathbb{F}}^2 \\ &\leq \frac{3}{8} \|\mathbf{M}\|^2 \cdot \left(2 \|\mathbf{M}^{\natural}\|^2 \|\Delta\|_{\mathbb{F}}^2 + \|\Delta\|_{\mathbb{F}}^4 \right) + \frac{1}{8} \|\mathbf{M}^{\natural}\|^2 \cdot \left\| \mathbf{M}^{\natural H} \mathbf{S} \Delta \right\|_{\mathbb{F}}^2,\end{aligned}$$

where step (a) follows from $\mathbf{M}^{\natural H} \mathbf{S} \mathbf{M}^{\natural} = \mathbf{0}$. Notice that $\|\mathbf{M}^{\natural}\| \leq \sqrt{2\sigma_1(\mathbf{Z}^{\natural})}$ and $\|\mathbf{M}\| \leq \|\mathbf{M} - \mathbf{M}^{\natural} \mathbf{Q}\|_{\mathbb{F}} + \|\mathbf{M}^{\natural}\| \leq \sqrt{\frac{\varepsilon^2 \sigma_r}{\mu_0 s}} + \sqrt{2\sigma_1}$. Thus we have

$$\begin{aligned}\|\nabla f_3\|_{\mathbb{F}}^2 &\leq \frac{3}{8} \left(\sqrt{\frac{\varepsilon^2 \sigma_r}{\mu_0 s}} + \sqrt{2\sigma_1} \right)^2 \cdot \left(4\sigma_1 + \frac{\varepsilon^2 \sigma_r}{\mu_0 s} \right) \|\Delta\|_{\mathbb{F}}^2 + \frac{1}{4} \sigma_1 \left\| \mathbf{M}^{\natural H} \mathbf{S} \Delta \right\|_{\mathbb{F}}^2 \\ &\leq \frac{3}{8} \cdot 2(\varepsilon^2 + 2)\sigma_1 \cdot (4 + \varepsilon^2)\sigma_1 \cdot \|\Delta\|_{\mathbb{F}}^2 + \frac{1}{4} \sigma_1 \left\| \mathbf{M}^{\natural H} \mathbf{S} \Delta \right\|_{\mathbb{F}}^2 \\ &\leq \frac{19}{4} \sigma_1^2 \cdot \|\Delta\|_{\mathbb{F}}^2 + \frac{1}{4} \sigma_1 \left\| \mathbf{M}^{\natural H} \mathbf{S} \Delta \right\|_{\mathbb{F}}^2,\end{aligned}\tag{6.27}$$

where the last line is due to $\varepsilon \leq \frac{1}{3}$.

Finally, plugging (6.25), (6.26) and (6.27) into (6.20), we obtain that

$$\begin{aligned}\|\nabla f(\mathbf{M})\|_{\mathbb{F}}^2 &\leq 4 \cdot 4(\mu_0 \mu s r \sigma)^2 \|\Delta\|_{\mathbb{F}}^2 + 4 \cdot 4(1+\varepsilon)^4 \sigma_1^2 \cdot \|\Delta\|_{\mathbb{F}}^2 + 2 \left(\frac{19}{4} \sigma_1^2 \cdot \|\Delta\|_{\mathbb{F}}^2 + \frac{1}{4} \sigma_1 \left\| \mathbf{M}^{\natural H} \mathbf{S} \Delta \right\|_{\mathbb{F}}^2 \right) \\ &\leq \left(64(\mu_0 \mu s r)^2 + 16(1+\varepsilon)^4 + \frac{19}{2} \right) \sigma_1^2 \|\Delta\|_{\mathbb{F}}^2 + \frac{1}{2} \sigma_1 \left\| \mathbf{M}^{\natural H} \mathbf{S} \Delta \right\|_{\mathbb{F}}^2 \\ &\leq 125(\mu_0 \mu s r \sigma_1)^2 \|\Delta\|_{\mathbb{F}}^2 + \frac{1}{2} \sigma_1 \left\| \mathbf{M}^{\natural H} \mathbf{S} \Delta \right\|_{\mathbb{F}}^2,\end{aligned}\tag{6.28}$$

where the second line is due to $\sigma \leq \frac{(1+\varepsilon)\sigma_1}{1-\varepsilon} \leq 2\sigma_1$ and the last line follows from $\varepsilon \leq \frac{1}{3} < 1$.

6.5 Auxiliary Lemmas

Lemma 6.5 ([33], Theorem 6.1). *Assume $\{\mathbf{X}_i\}_{i=1}^n$ are independent random matrices of dimension $n_1 \times n_2$ and obey $\mathbb{E}[\mathbf{X}_i] = 0$ and $\|\mathbf{X}_i\| \leq B$. Define*

$$\sigma^2 := \max \left\{ \left\| \mathbb{E} \left[\sum_{i=1}^n \mathbf{X}_i \mathbf{X}_i^H \right] \right\|, \left\| \mathbb{E} \left[\sum_{i=1}^n \mathbf{X}_i^H \mathbf{X}_i \right] \right\| \right\}.$$

Then the event

$$\left\| \sum_{i=1}^n \mathbf{X}_i \right\| \leq c \left(\sqrt{\sigma^2 \log(n_1 + n_2)} + B \log(n_1 + n_2) \right) \quad (6.29)$$

holds with probability at least $1 - (n_1 + n_2)^{-c_1}$, where $c, c_1 > 0$ are absolute constants.

Lemma 6.6 ([12], Lemma III.13). *Suppose \mathbf{Z}^\natural is μ_1 -incoherent. Then one has*

$$\begin{aligned} \sqrt{\sum_{i=0}^{n-1} \frac{\|\mathcal{G}^*(\mathbf{Z})\mathbf{e}_i\|_2^2}{\omega_i}} &\leq c_1 \sqrt{\frac{\mu_1 r \log(sn)}{n}} \sigma_1(\mathbf{Z}^\natural), \\ \max_{0 \leq i \leq n-1} \frac{\|\mathcal{G}^*(\mathbf{Z})\mathbf{e}_i\|_2}{\sqrt{\omega_i}} &\leq \frac{\mu_1 r}{n} \sigma_1(\mathbf{Z}^\natural). \end{aligned}$$

Lemma 6.7 ([12], Corollary III.9). *Under Assumption 1 and Assumption 2, let T be the tangent space of \mathbf{Z}^\natural , then the event*

$$\|\mathcal{P}_T \mathcal{G}(\mathcal{A}^* \mathcal{A} - \mathcal{I}) \mathcal{G}^* \mathcal{P}_T\| \leq c \sqrt{\frac{\mu_0 \mu_1 s r \log(sn)}{n}}$$

occurs with probability at least $1 - (sn)^{-c}$ for some universal constant $c > 0$.

7 Conclusion

In this paper, we propose a non-convex method called PGD-VHL for low rank vectorized Hankel matrix recovery problem in blind super-resolution of point sources. Our theoretical analysis shows that PGD-VHL converges to the target matrix linearly when the number of samples is larger than $\mathcal{O}(s^2 r^2 \log^2(sn))$. The performance of PGD-VHL has also been demonstrated by our numerical simulations. For future work, it is interesting to study the recovery performance of PGD-VHL in the presence of noise and the behavior of vanilla gradient descent method for blind super-resolution.

8 Acknowledgment

The authors would like to thank the anonymous reviewers and the Associate Editor for their useful comments which have helped to improve the quality of the present work. The authors also thank Ke Wei for helpful discussions.

References

- [1] Ali Ahmed, Benjamin Recht, and Justin Romberg. Blind deconvolution using convex programming. *IEEE Transactions on Information Theory*, 60(3):1711–1732, 2013.

- [2] Alan Barbieri, Giulio Colavolpe, Tommaso Foggi, Enrico Forestieri, and Giancarlo Prati. OFDM versus single-carrier transmission for 100 Gbps optical communication. *Journal of Lightwave Technology*, 28(17):2537–2551, 2010.
- [3] Christian R Berger, Bruno Demissie, Jörg Heckenbach, Peter Willett, and Shengli Zhou. Signal processing for passive radar using OFDM waveforms. *IEEE Journal of Selected Topics in Signal Processing*, 4(1):226–238, 2010.
- [4] Samuel Burer and Renato DC Monteiro. A nonlinear programming algorithm for solving semidefinite programs via low-rank factorization. *Mathematical Programming*, 95(2):329–357, 2003.
- [5] Jian-Feng Cai, Tianming Wang, and Ke Wei. Spectral compressed sensing via projected gradient descent. *SIAM Journal on Optimization*, 28(3):2625–2653, 2018.
- [6] Jian-Feng Cai, Tianming Wang, and Ke Wei. Fast and provable algorithms for spectrally sparse signal reconstruction via low-rank Hankel matrix completion. *Applied and Computational Harmonic Analysis*, 46(1):94–121, 2019.
- [7] Emmanuel J Candès and Carlos Fernandez-Granda. Super-resolution from noisy data. *Journal of Fourier Analysis and Applications*, 19(6):1229–1254, 2013.
- [8] Emmanuel J Candès and Carlos Fernandez-Granda. Towards a mathematical theory of super-resolution. *Communications on pure and applied Mathematics*, 67(6):906–956, 2014.
- [9] Emmanuel J Candes, Xiaodong Li, and Mahdi Soltanolkotabi. Phase retrieval via wirtinger flow: Theory and algorithms. *IEEE Transactions on Information Theory*, 61(4):1985–2007, 2015.
- [10] Emmanuel J Candes and Yaniv Plan. A probabilistic and RIPless theory of compressed sensing. *IEEE Transactions on Information Theory*, 57(11):7235–7254, 2011.
- [11] Emmanuel J Candès and Benjamin Recht. Exact matrix completion via convex optimization. *Foundations of Computational Mathematics*, 9(6):717, 2009.
- [12] Jinchi Chen, Weiguo Gao, Sihan Mao, and Ke Wei. Vectorized Hankel lift: A convex approach for blind super-resolution of point sources. *arXiv preprint arXiv:2008.05092*, 2020.
- [13] Yudong Chen and Yuejie Chi. Harnessing structures in big data via guaranteed low-rank matrix estimation: Recent theory and fast algorithms via convex and nonconvex optimization. *IEEE Signal Processing Magazine*, 35(4):14–31, 2018.
- [14] Yudong Chen and Martin J Wainwright. Fast low-rank estimation by projected gradient descent: General statistical and algorithmic guarantees. *arXiv preprint arXiv:1509.03025*, 2015.
- [15] Yuejie Chi. Guaranteed blind sparse spikes deconvolution via lifting and convex optimization. *IEEE Journal of Selected Topics in Signal Processing*, 10(4):782–794, 2016.
- [16] Yuejie Chi, Yue M Lu, and Yuxin Chen. Nonconvex optimization meets low-rank matrix factorization: An overview. *IEEE Transactions on Signal Processing*, 67(20):5239–5269, 2019.
- [17] James Everett Evans, DF Sun, and JR Johnson. Application of advanced signal processing techniques to angle of arrival estimation in atc navigation and surveillance systems. Technical report, Massachusetts Inst of Tech Lexington Lincoln Lab, 1982.
- [18] JE Evans. High resolution angular spectrum estimation technique for terrain scattering analysis and angle of arrival estimation. In *1st IEEE ASSP Workshop Spectral Estim., McMaster Univ., Hamilton, Ont., Canada, 1981*, pages 134–139, 1981.

- [19] Michael Grant and Stephen Boyd. CVX: MATLAB software for disciplined convex programming, version 2.1. <http://cvxr.com/cvx>, March 2014.
- [20] Prateek Jain, Purushottam Kar, et al. Non-convex optimization for machine learning. *Foundations and Trends® in Machine Learning*, 10(3-4):142–336, 2017.
- [21] Shuang Li, Michael B Wakin, and Gongguo Tang. Atomic norm denoising for complex exponentials with unknown waveform modulations. *IEEE Transactions on Information Theory*, 66(6):3893–3913, 2019.
- [22] Xiaodong Li, Shuyang Ling, Thomas Strohmer, and Ke Wei. Rapid, robust, and reliable blind deconvolution via nonconvex optimization. *Applied and computational harmonic analysis*, 47(3):893–934, 2019.
- [23] Xiliang Luo and Georgios B Giannakis. Low-complexity blind synchronization and demodulation for (ultra-) wideband multi-user ad hoc access. *IEEE Transactions on Wireless communications*, 5(7):1930–1941, 2006.
- [24] Sihan Mao and Jinchi Chen. Blind super-resolution via projected gradient descent. *arXiv preprint arXiv:2110.02478*, 2021.
- [25] Gary F Margrave, Michael P Lamoureux, and David C Henley. Gabor deconvolution: Estimating reflectivity by nonstationary deconvolution of seismic data. *Geophysics*, 76(3):W15–W30, 2011.
- [26] Leandro Pralon, Gabriel Beltrao, Alisson Barreto, and Bruno Cosenza. On the analysis of PM/FM noise radar waveforms considering modulating signals with varied stochastic properties. *Sensors*, 21(5):1727, 2021.
- [27] Xiaobo Qu, Maxim Mayzel, Jian-Feng Cai, Zhong Chen, and Vladislav Orekhov. Accelerated NMR spectroscopy with low-rank reconstruction. *Angewandte Chemie International Edition*, 54(3):852–854, 2015.
- [28] Sean Quirin, Sri Rama Prasanna Pavani, and Rafael Piestun. Optimal 3D single-molecule localization for superresolution microscopy with aberrations and engineered point spread functions. *Proceedings of the National Academy of Sciences*, 109(3):675–679, 2012.
- [29] Yoav Shechtman, Yonina C Eldar, Oren Cohen, Henry Nicholas Chapman, Jianwei Miao, and Mordechai Segev. Phase retrieval with application to optical imaging: A contemporary overview. *IEEE signal processing magazine*, 32(3):87–109, 2015.
- [30] Mohamed A Suliman and Wei Dai. Blind two-dimensional super-resolution and its performance guarantee. *arXiv preprint arXiv:1811.02070*, 2018.
- [31] Mohamed A Suliman and Wei Dai. Mathematical theory of atomic norm denoising in blind two-dimensional super-resolution. *IEEE Transactions on Signal Processing*, 69:1681–1696, 2021.
- [32] Kim-Chuan Toh, Michael J Todd, and Reha H Tütüncü. SDPT3—a MATLAB software package for semidefinite programming, version 1.3. *Optimization methods and software*, 11(1-4):545–581, 1999.
- [33] Joel A Tropp. User-friendly tail bounds for sums of random matrices. *Foundations of computational mathematics*, 12(4):389–434, 2012.
- [34] Stephen Tu, Ross Boczar, Max Simchowitz, Mahdi Soltanolkotabi, and Ben Recht. Low-rank solutions of linear matrix equations via procrustes flow. In *International Conference on Machine Learning*, pages 964–973. PMLR, 2016.

- [35] Edwin Vargas, Kumar Vijay Mishra, Roman Jacome, Brian M Sadler, and Henry Arguello. Joint radar-communications processing from a dual-blind deconvolution perspective. In *ICASSP 2022-2022 IEEE International Conference on Acoustics, Speech and Signal Processing (ICASSP)*, pages 5622–5626. IEEE, 2022.
- [36] Ke Wei, Jian-Feng Cai, Tony F Chan, and Shingyu Leung. Guarantees of Riemannian optimization for low rank matrix recovery. *SIAM Journal on Matrix Analysis and Applications*, 37(3):1198–1222, 2016.
- [37] Dehui Yang, Gongguo Tang, and Michael B Wakin. Super-resolution of complex exponentials from modulations with unknown waveforms. *IEEE Transactions on Information Theory*, 62(10):5809–5830, 2016.
- [38] Zai Yang, Jian Li, Petre Stoica, and Lihua Xie. Sparse methods for direction-of-arrival estimation. In Rama Chellappa and Sergios Theodoridis, editors, *Academic Press Library in Signal Processing, Volume 7*, pages 509–581. Elsevier, 2018.
- [39] Zai Yang, Petre Stoica, and Jinhui Tang. Source resolvability of spatial-smoothing-based subspace methods: A hadamard product perspective. *IEEE Transactions on Signal Processing*, 67(10):2543–2553, 2019.
- [40] Shuai Zhang, Yingshuai Hao, Meng Wang, and Joe H Chow. Multichannel Hankel matrix completion through nonconvex optimization. *IEEE Journal of Selected Topics in Signal Processing*, 12(4):617–632, 2018.
- [41] Le Zheng and Xiaodong Wang. Super-resolution delay-Doppler estimation for OFDM passive radar. *IEEE Transactions on Signal Processing*, 65(9):2197–2210, 2017.
- [42] Qinqing Zheng and John Lafferty. Convergence analysis for rectangular matrix completion using Burer–Monteiro factorization and gradient descent. *arXiv preprint arXiv:1605.07051*, 2016.
- [43] Zengying Zhu, Jinchi Chen, and Weiguo Gao. Low rank vectorized Hankel lift for matrix recovery via fast iterative hard thresholding. *arXiv preprint arXiv:2109.11414*, 2021.